Title

Salmonella Typhimurium employs spermidine to exert protection against ROS-mediated cytotoxicity and rewires host polyamine metabolism to ameliorate its survival in macrophages**.**

Abhilash Vijay Nair[a], Anmol Singh[a], R. S. Rajmani[b], Dipshikha Chakravortty[a,c]#

[a]Department of Microbiology and Cell Biology, Division of Biological Sciences, Indian Institute of Science, Bengaluru, India

[b]Molecular Biophysics Unit, Indian Institute of Science, Bangalore, India

[c]Adjunct Faculty, School of Biology, Indian Institute of Science Education and Research, Thiruvananthapuram

#Address correspondence to Dipshikha Chakravortty, dipa@iisc.ac.in, Tel: 0091 80 2293 2842, Fax: 0091 80 2360 269

Keywords: Antioxidative response, D, L-α-difluoromethylornithine, Glutathionyl-spermidine synthetase, Macrophages, Spermidine

Abstract

Salmonella infection entails a cascade of attacks and defence measures. After breaching the intestinal epithelial barrier, *Salmonella* is phagocytosed by macrophages, where the bacteria encounter multiple stresses, to which it employs relevant countermeasures. Our study shows that, in *Salmonella*, the polyamine spermidine activates a stress response mechanism by regulating critical antioxidant genes. *Salmonella* Typhimurium mutants for spermidine transport and synthesis cannot mount an antioxidative response, resulting in high intracellular ROS levels. These mutants are also compromised in their ability to be phagocytosed by macrophages. Furthermore, it regulates a novel enzyme in *Salmonella*, Glutathionyl-spermidine synthetase (GspSA), which prevents the oxidation of proteins in *E. coli*. Moreover, the spermidine mutants and the GspSA mutant show significantly reduced survival in the presence of hydrogen peroxide *in vitro* and reduced organ burden in the mouse model of *Salmonella* infection. Conversely, in macrophages isolated from *gp91phox*$^{-/-}$ mice, we observed a rescue in the attenuated fold proliferation previously observed upon infection. We found that *Salmonella* upregulates polyamine biosynthesis in the host through its effectors from SPI-1 and SPI-2, which addresses the attenuated proliferation observed in spermidine transport mutants. Thus, inhibition of this pathway in the host abrogates the proliferation of *Salmonella* Typhimurium in macrophages. From a therapeutic perspective, inhibiting host polyamine biosynthesis using an FDA-approved chemopreventive drug, D, L-α-difluoromethylornithine (DFMO), reduces *Salmonella* colonization and tissue damage in the mouse model of infection while enhancing the survival of infected mice. Therefore, our work provides a mechanistic insight into the critical role of spermidine in stress resistance of *Salmonella*. It also reveals a bacterial strategy in modulating host metabolism to promote their intracellular survival and shows the potential of DFMO to curb S*almonella* infection.

Introduction

An optimal microbial growth condition has signatures of ample nutrients and ambient temperature, pH, oxygen concentration, and osmolarity. Any disturbances in one or more of these parameters can be tagged as a stress condition, detrimental to microbial survival and growth. Given the fluctuations of these parameters are nature-driven (1), the microbes need to be adept at sensing, responding, and adapting to unprecedented situations (2). Food-borne pathogens deal with an array of stresses in their dwelling environments, stemming from natural to commercial causes and host systems.(3-5). *Salmonella* is a food-borne pathogen that enters the host system through contaminated food and water. While travelling to the intestine, *Salmonella* faces multiple stressful conditions such as low pH, nutrient deprivation, bile salt stress, competition with the resident microbes of the gut and immunoglobulins, etc. Once it breaches the epithelial barrier, it is taken up by the macrophages at the lamina propria, through which it disseminates throughout the host system. Entry of the pathogen into the macrophage leads to a burst of reactive oxygen species (ROS) generated by the NADPH phagocytic oxidase (Nox2) and reactive nitrogen species (RNS) generated majorly by inducible Nitric Oxide synthase (Nos2) (6, 7). In macrophages, *Salmonella* resides in a specialized niche called the *Salmonella*-containing vacuole (SCV), which presents multiple other stresses to the bacteria, such as acidification, nutrient limitation, and attack by the antimicrobial peptides. However, *Salmonella* employs numerous weapons from its arsenal to counteract those stresses.

Polyamines are a group of primordial stress response molecules in prokaryotes and eukaryotes (8). Multiple research groups have elucidated the link between polyamines and bacterial stress response. In *Shigella spp.* the polyamine spermidine accumulates during its infection into

macrophages, which increases the expression of *katG* and helps in bacterial antioxidant response (9). Another study demonstrated that spermidine localises to the surface of *Pseudomonas aeruginosa* and binds to the lipopolysaccharide (LPS) to protect the cells from oxidative damage (10). In the Gram-positive bacteria *Streptococcus pyogenes,* extracellular spermidine enhances the survival of the bacteria by upregulating oxidative response genes (11). Espinel IC *et.al*, has shown that polyamines are vital in resistance against nitrosative stress in *Salmonella* Typhimurium. Further, the group showed that spermidine is required for the systemic infection of *Salmonella* Typhimurium in mice (12). Our previous studies further indicated that *Salmonella* upregulates the spermidine transporter genes (*potA, potB, potC* and *potD*) and the biosynthesis genes (*speE* and *speD*) during the log phase of growth *in vitro* (13, 14). Thus, it can be inferred that *Salmonella* Typhimurium utilises polyamines, such as spermidine, as a stress response molecule.

Objective

The research in *Salmonella* shows that polyamines are stress response molecules, but the mechanism behind the process remains elusive. We wanted to decipher the mechanism, and the molecular players involved in the stress response pathways regulated by spermidine in *Salmonella.* Here, we show that spermidine biosynthesis and transport mutants of *Salmonella* Typhimurium exhibit reduced survival upon infection in RAW264.7 cells. This diminished proliferation is also observed in mice models of *Salmonella* infection, which is rescued in *gp91phox*$^{-/-}$ mice. We demonstrate that spermidine manipulates the various arms of antioxidative response and tightly regulates intracellular ROS levels. We further identify a novel antioxidative enzyme, GspSA, in *Salmonella* Typhimurium, which is regulated by spermidine. The primary question that remains is why the transporter mutant shows reduced survival. To this, we find that *Salmonella* Typhimurium harnesses the host polyamine biosynthesis for its survival. Furthermore, for the first time, we show

that an FDA-approved chemopreventive and anti-African Human Trypanosomiasis drug that inhibits polyamine biosynthesis in the host can curb *Salmonella* infection in mice.

Material and Methods

Bacterial strains and growth condition

Salmonella enterica serovars Typhimurium (STM WT) wild-type strain ATCC 14028s was used in all experiments, which was a kind gift from Prof. Michael Hensel, Abteilung Mikrobiologie, Universität Osnabrück, 273 Osnabrück, Germany. The bacterial strain was cultured in Luria broth (LB-Himedia) with constant shaking (175rpm) at 37°C orbital-shaker. Kanamycin, Chloramphenicol and Ampicillin antibiotics (Final working concentrations of Kanamycin-50µg/ml, Cholramphenicol-20µg/ml and Ampicillin-50µg/ml) were used wherever required. Strains were transformed with a pFPV-m-cherry plasmid for immunofluorescence assays. For the supplementation study, the bacterial strains were grown in Luria broth with 100µM spermidine (Sigma) addition with constant shaking (175rpm) at 37°C orbital-shaker overnight. (Bacterial strain list in Supplementary table **S-Table 1**)

Bacterial gene knock-out and strain generation

The generation of gene knockout in bacteria was done using the One-step chromosomal gene inactivation protocol based on the principle of homologous recombination (15). The plasmids pKD4 and pKD3 serve as a template for amplifying the Kanamycin resistance gene (Kan^R) and the Chloramphenicol resistance gene ($Chlm^R$). Briefly, the Kanamycin resistance gene (Kan^R) and the Chloramphenicol resistance gene ($Chlm^R$) amplified products were purified using chloroform-ethanol precipitation. The Kan^R was used to generate STM *ΔpotCD* (*pot*- spermidine transporter mutant), and $Chlm^R$ was used to generate STM *ΔspeED* (*spe*-spermidine biosynthesis mutant).

This was followed by electroporation into the STM WT cells expressing pKD-46 plasmid, which provides the λ-Red recombinase system required for the homologous recombination. The electroporation was carried out by applying a single pulse of 2.25 kV for each sample. The transformant colonies were selected and patched on fresh plates with the required antibiotic for a further selection of the transformants and confirmed for knockout using PCR with primers designed corresponding to the ~100bp upstream and downstream of the genes (knocked out) for the knockout strains to observe a difference in PCR product size upon STM *ΔpotCD* and STM *ΔspeED* knockout generation. For the generation of the double knock-out strain (STM *ΔpotCDΔspeED,* spermidine transporter and biosynthesis double mutant), the STM *ΔpotCD* (resistant to Kanamycin) was first transformed with the plasmid pKD46, which provides the λ-Red recombinase system. To this transformed strain, the purified PCR product to knock-out *speED* was electroporated to generate the STM *ΔpotCDΔspeED* (resistant to Kanamycin and Chloramphenicol). For the generation of STM *Δgsp* (glutathionyl-spermidine synthetase mutant), the Kanamycin resistance gene was amplified from pKD4 plasmid, and a similar protocol was used, followed by selection on Kanamycin containing LB agar plates. To generate double gsp spermidine mutants, STM *Δgsp* was electroporated with purified PCR product to knock out *speED* and *potCD* (both Chloramphenicol resistance cassettes). (Knock-out generation Primer list in Supplementary table **S-Table 2**)

Cell culture and maintenance

RAW264.7 cells (murine macrophage cell line) were cultured in DMEM - Dulbecco's Modified Eagle Medium (Lonza) supplemented with 10% FBS (Gibco) and 1% Penicillin-streptomycin (Sigma- Aldrich) at 37°C humidified chamber (Panasonic) with 5% CO_2. For each experiment, the

cells were seeded onto the appropriate cell culture well plate at a confluency of 80% for intracellular survival assay and expression studies.

Gentamicin protection assay

The cells were infected with STM WT, STM *ΔpotCD,* STM *ΔspeED,* STM *ΔpotCDΔspeED,* STM *Δgsp* and STM *ΔkatG* (all strains were grown overnight in LB medium) at Multiplicity of Infection (MOI) of 10 (for intracellular survival assay) and MOI 25 (for qRT-PCR). After infecting the cell line with STM WT and the mutants, the plate was centrifuged at 900 rpm (100xg) (Rota-Superspin R-NV swing bucket centrifuge) for 10 minutes to facilitate the proper adhesion. The plate was then incubated for 25 minutes at 37°C in a humidified chamber and 5% CO_2. Then, the media was removed from the wells and washed with 1X PBS. Fresh media containing 100 µg/mL gentamicin was added and incubated for 60 minutes at 37°C and 5% CO_2. The media was removed, cells were washed with 1X PBS twice, and fresh media containing 25µg/mL gentamicin was added. The plate was incubated at 37°C and 5% CO_2 till the appropriate time. For the intracellular survival assay, two time points were considered 2 hours and 16 hours; for qRT-PCR, three time points were considered 2 hours, 6 hours, and 16 hours.

For the Opsonisation assay, the overnight grown bacterial strains were washed with 1XPBS. The washed cells (for each strain) were treated with the opsonin, here mouse complement sera, for 1 hour at 37°C. Mouse complement-sera acts as an opsonin and thus potentiates the interaction of the bacteria with the macrophages. The treated bacterial strains were then used for infection into RAW264.7 macrophages at MOI of 50 as per the described gentamicin protection assay above and the percentage phagocytosis was determined (16).

Also, for studying the effect of exogenous spermidine in the recovery of the phenotype of mutant strains, the strains were grown *in vitro* with supplementation of 100μM spermidine (described previously in the "Bacterial strains and growth" section). The grown cultures were then used for infection of RAW264.7 cells using the gentamicin protection assay.

Intracellular survival assay and phagocytosis assay

At the appropriate time post-infection, the cells were lysed using 0.1% Triton X, followed by adding more 1X PBS and samples were collected. The collected samples were plated at the required dilutions on LB agar plates and kept at 37°C. Twelve hours post incubation, the Colony forming units (CFU) were enumerated for each plate.

The fold proliferation and invasion were determined as follows:

Fold Proliferation = (CFU at 16 hours post-infection)/(CFU at 2 hours post-infection)

Percentage Phagocytosis = [(CFU at 2 hours post-infection)/(CFU of the Pre-inoculum)]×100

RNA isolation and qRT-PCR

RNA isolation was performed from infected cells after appropriate hours of infection with STM WT, STM *ΔpotCD, and* STM *ΔspeED* by RNA isolation using TRIzol (from TaKaRa, RNA isoPlus-9109) reagent according to the manufacturer's protocol. RNA was quantified using Thermo-fisher scientific Nano Drop followed by running on 2% agarose gel to check the quality. For cDNA synthesis, the first DNase I treatment with 3μg of isolated RNA was done at 37℃ for 60 minutes, which was then stopped by heating at 65℃ for 10 minutes. Then RNA (free of DNA) was subjected to Reverse transcription using Random hexamer, 5X RT buffer, RT enzyme, dNTPs, and DEPC treated water at 37°C for 15 minutes, followed by heating at 85℃ for 15 as per

manufacturer's protocol (from TaKaRa, PrimeScript RTKit-RR037A). Quantitative real-time PCR was done using the SYBR green RT-PCR kit in the BioRad qRT-PCR system (BioRad CFX96 Touch Real-Time PCR Detection System). A 384-well plate with three replicates for each sample was used. The gene expression levels of interest were measured using specific RT primers. Gene expression levels were normalised to 16SrRNA primers of *S.* Typhimurium. Gene expression levels of the eukaryotic gene of interest were normalised to beta-actin of mouse/human as required. (Expression Primer list in Supplementary table **S-Table 2**).

For expression studies in bacteria grown in LB media, the bacterial samples were harvested at 3 hours, 6 hours, 9 hours, and 12 hours post subculture in fresh LB media in a 1:100 ratio, and 1mM H_2O_2 was added to the broth to study the gene expression in the presence of oxidative stress. Then, a similar protocol was used to isolate total RNA using TRIzol (from TaKaRa, RNA isoPlus-9109) reagent according to the manufacturer's protocol (Expression Primer list in Supplementary table **S-Table 2**).

For expression studies in the liver and spleen, the tissues from the respective organs were collected in TRIzol (from TaKaRa, RNA isoPlus-9109), five days post oral gavage of 10^7 CFU of STM WT bacteria. The tissues were homogenized using 1mm Glass beads in a Bead-beater (BioSpec products). The homogenized lysate was collected, and total RNA isolation and cDNA preparation were performed as previously described (Expression Primer list in Supplementary table **S-Table 2**).

Primary macrophage isolation and infection

Primary macrophages were isolated using a previously established protocol (17, 18) from C57BL/6J mice (The Jackson's Laboratory, USA, male, 5-6 weeks old), *gp91phox* knockout mice

and *iNOS* knockout mice (all knock-out mice are in C57BL/6J background procured from The Jackson's Laboratory, USA). The mice were intraperitoneally injected with 8% Brewer's Thioglycolate (from HiMedia). Five days post-injection, the primary macrophages were isolated by injecting ice-cold 1xPBS into the peritoneal cavity, and the peritoneal lavage was collected. Any residual erythrocytes were lysed using an RBC lysis buffer (Sigma- R7757), and the isolated cells were maintained in a complete RPMI 1640 medium for further experiments.

Intracellular Reactive oxygen species determination using H_2DCFDA staining

Overnight cultures were sub-cultured in fresh LB media. Once the cultures reached OD 0.1 then, 10^8 CFU/ml of each strain was incubated with 10µM of 2',7'-dichlorodihydrofluorescein diacetate (H2DCFDA) (Sigma) in 1xPBS (pH 7.2) at 37°C for 30 minutes. The bacterial cells were centrifuged, and the cells were resuspended in 1xPBS (pH 7.2) with Hydrogen peroxide of different concentrations (0- 10mM) and incubated at 37°C (orbital shaker) for 2 hours. The samples were transferred to a 96-well ELISA plate, and fluorescence was determined in Tecan-ELISA plate reader Infinite series 200 (Ex- 490nm/ Em- 520nm).

Intracellular redox status determination

The STM WT, STM *ΔpotCD,* STM *ΔspeED* and STM *Δgsp* were transformed with pQE60-Grx1-roGFP2 (a gift from Prof. Amit Singh, CIDR, IISc). roGFP2 is a genetically modified form of GFP (GFP ex 488nm) that harbours two cysteine residues, and upon oxidation, the cysteine residues form a disulphide bond, and the excitation shifts to 408nm (19, 20). Briefly, overnight cultures were subcultured in fresh LB media (with 500µM IPTG to induce roGFP2). Once the cultures reached OD 0.1 then, 10^8 CFU/ml of each strain was incubated with Hydrogen peroxide (0mM-5mM) of different concentrations in 1XPBS (pH 7.2) with and incubated 37°C (orbital shaker) for

2 hours. The samples were centrifuged and resuspended in fresh 1XPBS (pH 7.2). Tubes were analysed for GFP fluorescence at 408nm and 488nm, respectively, using a BD-FACS Verse flow cytometer (total of 10,000 events for each sample). We have measured fluorescence intensity at 408nm and 488nm for each sample. During quantification, we gated for the live cells (P1), followed by the singlet population (P2), followed by 488nm (P3) and then 408nm channel (P4). Finally, we enumerated the ratio of the mean intensity at 408nm to 488nm from the final gated population (P4) for each sample. The higher intensity at 408nm represents an oxidative environment. Thus, the ratio of 408/488 determines the degree of oxidation. Higher intensity at 408nm indicates an oxidative environment. To determine intracellular redox status upon infection into RAW264.7 cells, 10^5 RAW264.7 cells seeded in a 24-well tissue culture plate were infected with each strain harbouring the roGFP2(induced with IPTG similarly) plasmid using gentamicin protection assay. After 16 hours post-infection, the macrophages were washed with 1X PBS and scrapped off using a cell scraper and analysed for GFP fluorescence at 408nm and 488nm, respectively, using BD-FACS Verse flow cytometer (total 10,000 events for each sample). As previously explained, we quantified the mean fluorescence intensity at 488nm and 408nm for each sample. Then we enumerated the ratio of the mean intensity at 408nm to 488nm from the final gated population (P4) for each sample. Higher intensity at 408nm indicates an oxidative environment.

***In vitro* sensitivity assays**

Overnight cultures were sub-cultured in fresh LB media. Once the cultures reached OD 0.1 then 10^8 CFU/ml of each strain was incubated with Hydrogen peroxide of different concentrations (0mM- 10mM) in 1XPBS (pH 7.2) and incubated 37°C (orbital shaker) for 2 hours. The samples

were plated on SS agar to enumerate the CFU, and the percentage survival was determined as follows:

Percentage Survival: [[CFU/ml for treated with H_2O_2/ $NaNO_2$]/ [CFU/ml for untreated]]×100

The bacterial samples were prepared to determine the nitrite sensitivity, similar to the hydrogen peroxide sensitivity assay described above. Each strain was incubated with sodium nitrite (0mM-10mM) in 1xPBS of pH 5.4 to facilitate dissociation into nitrite ions and incubated 37°C (orbital shaker) for 2 hours. The samples were plated on SS agar to enumerate the CFU, and the percentage survival was determined as previously described for hydrogen peroxide sensitivity assays. For dual hydrogen peroxide and sodium nitrite assays, the strains were incubated with both hydrogen peroxide and sodium nitrite (0mM- 10mM concentrations of each stress molecule).

Resazurin assay was used to determine the viable cells and was performed in 96 well plates (triplicate for each sample and concentration. Briefly, after incubation for 2 hours as previously performed, Resazurin (0.2mg/ml in 1X PBS) was added (1:10 ratio) to each well of 96 well plates. The plate was incubated at 37°C in a shaker incubator for 2 hours. The fluorescence was measured using a Tecan plate reader infinite series 200, with Ex-520nm and Em- 590nm. The values were obtained as Relative fluorescence units (RFU), and the percentage survival was determined as

Percentage survival = [RFU of the sample with added hydrogen peroxide]/ [RFU of the sample without hydrogen peroxide]

Immunoblotting

The bacterial strains were grown in LB media with added 1mM hydrogen peroxide until the log phase of growth. The cells were centrifuged to remove the media, and the cells were resuspended in the lysis buffer (Sodium chloride, Tris, EDTA, 10% protease inhibitor cocktail (Roche,

04693116001)) after washing with 1XPBS. The cells were lysed using sonication and centrifuged at 4°C to collect the cell lysate, followed by estimation of total protein using the Bradford protein estimation method. 50µg of protein was loaded onto a Polyacrylamide Gel Electrophoresis (PAGE) (12% Resolving gel) without β-mercaptoethanol (prevent di-sulphide bond breakage as glutathionyl-spermidine modifies Cysteine residues through a disulphide bond), then transferred onto 0.45µm PVDF membrane (GE Healthcare). 5% skimmed milk (Hi-Media) in TBST was used to block for 1 hour at room temperature and then probed with Anti-Spermidine primary (Novus Biologicals, NB100-1847, 1:2000 dilution in 2.5% BSA) and secondary HRP-conjugated antibody (anti-rabbit IgG HRP linked Cell Signaling Technology #7074, 1:2000 dilution in 2.5% BSA). ECL (BioRad) was used to develop the blot, and images were captured using Chemi-Doc (BioRad). All densitometric analysis was performed using Image J. The normalisation was done with respect to the Ponceau S stained blot.

For studying the expression on iNOS, the RAW264.7 macrophages were washed with PBS and collected using cell scrapper, after infection with STM WT (MOI 10). The cells were centrifuged at 300g at 4°C for 10 minutes. The cells were resuspended in RIPA lysis buffer supplemented with 10% protease inhibitor cocktail (Roche, 04693116001) and incubated on ice for 30 minutes. Total protein was estimated using Bradford estimation. 100µg of the protein samples were loaded onto a Polyacrylamide Gel Electrophoresis (PAGE) (8% Resolving gel for larger size of iNOS). Then transferred onto 0.45µm PVDF membrane (GE Healthcare). 5% skimmed milk (Hi-Media) in TBST was used to block for 1 hour at room temperature followed by probing with Anti-iNOS antibody (Sigma, SAB4502011, 1:1000 dilution in 2.5% BSA) and HRP-conjugated antibody (anti-rabbit IgG HRP linked Cell Signaling Technology #7074, 1:2000 dilution in 2.5% BSA).

ECL (BioRad) was used to develop the blot, and images were captured using Chemi-Doc (BioRad). All densitometric analysis was performed using Image J.

Transfection for knockdown

To ensure maximum knockdown, we have targeted the 3'-UTR of Odc1 and Srm from mouse. We used CLUSTAL OMEGA to align and identify the 3'-UTR complementary regions. We chose two sequences for each gene. For transfection, RAW 264.7 cells were seeded at a 50-60% confluency 12 hours before transfecting using PEI (1:2 -DNA: PEI) (18, 21). We used the two different constructs for the knockdown of Odc1, A7 and A8 and both as a mixed construct (A7:A8 at 1:1 ratio) and similarly for Srm, E9 and F1 and both as a mixed construct (E9:F1 at 1:1 ratio) from the Sigma Mission shRNA library. 400ng of plasmid DNA/well (ratio 260/280 ~1.8- 1.9) was used for transfection in a 24well plate. Cells were then incubated for 8 hours at 37℃ in a humidified incubator with 5%CO_2; after that, the media containing transfecting DNA and reagents were removed, and cells were further incubated for 48 hours in complete media DMEM +10% FBS. Cells were harvested for further analysis or infected with the required MOI using the gentamicin protection assay. (shRNA sequence list in Supplementary table **S-Table 3**)

Immunofluorescence

After the appropriate incubation time after the gentamicin protection assay, the media was removed, and the cells were washed with 1XPBS and fixed with 3.5% Paraformaldehyde for 10 minutes. The cells were washed with 1XPBS, incubated with the required primary antibodies [anti-mouseLAMP1(1:100 dilution) and anti-Spermidine (anti-spermidine Novus Biologicals, NB100-1847, 1:100 dilution)] in a buffer containing 0.01% saponin and 2% BSA, and incubated at room temperature for 45-60 minutes. After washing with 1XPBS, the secondary antibody tagged to a

fluorochrome was added and incubated [anti-rat-Alexafluor488(#112-547-003 Jacksons Immunoresearch Lab Inc. 1:200 dilution) for LAMP1, anti-rabbit-Alexafluor647(SIGMA-ALDRICH Antibody-CF647, 1:200 dilution) for spermidine]. The coverslips were then washed with PBS and mounted on a clean glass slide using mounting media containing an anti-fade reagent and observed under the confocal microscope (Zeiss 710 microscope, at 63X oil immersion, 2X319 3X zoom, and 100X zoom for studying only bacterial samples, Zeiss 880 microscope, at 63X oil immersion, 2X319 3x zoom).

The histopathological sections were deparaffinized by washing in Xylene for 10 minutes, followed by absolute ethanol for 5 minutes, followed by washes in 95% ethanol and 70% ethanol for 2 minutes each. Finally, after a wash in water, the slides were heated in Tris-EDTA buffer (pH 9.0, 10mM Tris, 1mM EDTA) for 2 minutes (microwave used) for antigen retrieval. The dried slides were then incubated with the required primary antibody (anti- *Salmonella* LPS, Sigma #SAB4200862, 1:200) in a buffer containing 0.01% saponin and 2% BSA (for blocking) and incubated at room temperature for 45-60 minutes. The primary antibody was removed by washing with 1XPBS and then incubated with the appropriate secondary antibody tagged to a fluorochrome. The sections were washed with 1XPBS and covered with coverslip after using mounting media containing an anti-fade reagent. The coverslips were sealed with clear nail polish and observed under the confocal microscope. Zeiss 880 microscope 40X oil immersion 2X319 3X zoom was used to study histopathology samples.

Intracellular RNS determination

To determine intracellular RNS, a cell-permeable nitric-oxide probe, 4, 5- Diaminofluorescein diacetate (DAF_2A) (Sigma, #D225), was used. The protocol has been modified from Roy Chowdhury et al. 2022 (22). RAW264.7 cells were infected with STM WT at MOI-10 as per the

gentamicin protection assay. Here, D, L-α-difluoromethylornithine (DFMO Sigma #D193, at 5μM) and IFNγ (Invitrogen, # BMS326, at 20ng/μL) and 1400W dihydrochloride (iNOS inhibitor, Sigma #W4262, at 5μM) treatment was given with 25μg/mL gentamicin. After 16 hours of infection and incubation, the cells were then incubated with fresh DMEM containing 5μM of DAF_2DA. The cells were incubated at 37°C in a humidified incubator with 5% CO_2 for 30 minutes. The media containing dye was removed, the cells were washed with 1XPBS, and the cells were acquired immediately for flow cytometry (BD FACS Verse) (Ex- 491nm/Em- 513nm).

Intracellular Glutathione determination

The intracellular reduced Glutathione (GSH) concentration was determined by modification of a published protocol (23). Briefly, a standard curve with the known concentration of GSH (Sigma) was prepared. The reaction mixture for each contained 600μL of phosphate buffer (0.1M, pH7), 40μL of 0.4% w/v 5,5-dithiobis(2-nitrobenzoic acid) (DTNB, from Sigma), 100 μL of the standard solutions of GSH (0mM-1mM range) and autoclaved MilliQ water to make up the volume to 1000μL. The mixture was incubated at room temperature for 5 minutes, and absorbance was measured at 412nm using a tecan plate reader. The bacterial strains were subcultured in fresh LB media and grown till OD 0.1 (exponential phase), washed with buffer (Tris, Sodium chloride and EDTA) and lysed using sonication. The supernatant was used as the sample for GSH detection after sonication. As previously described for the standard curve. From the standard curve, the intracellular concentrations were interpolated.

***In silico* analysis**

The *in silico* protein structure determination was performed using the SWISS-MODEL software (https://swissmodel.expasy.org/), where we supplied the protein sequence of GspSA of

Salmonella Typhimurium from UniProt. We analysed the model with the highest sequence identity and maximum coverage with the Gsp from *E. coli*. The structure depicts a Homo dimer with a GMQE of 0.93 and QMEANisCo Global of 0.88 ± 0.05.

***In vivo* animal experiment**

5-6weeks old C57BL/6J mice were infected by orally gavaging 10^7 CFU of STM WT, STM *ΔpotCD,* STM *ΔspeED,* STM *ΔpotCDΔspeED,* STM *Δgsp* and STM *ΔkatG*. To study the colonisation in organs, the intestine (Peyer's patches), MLN, spleen and liver were isolated aseptically (in Biosafety level -2 cabinet), 5 days post-infection, and the CFU was enumerated on differential and selective SS agar by serial dilution. For intraperitoneal infection, 5-6weeks old C57BL/6J mice were infected by intraperitoneally injecting 10^3 CFU of STM WT, STM *ΔpotCD,* STM *ΔspeED,* STM *ΔpotCDΔspeED,* STM *Δgsp* and STM *ΔkatG.* The spleen and liver were isolated aseptically 3 days post-infection to study the colonisation in organs. Blood was isolated by heart puncture 3 days post-infection. The CFU was enumerated on differential and selective SS agar by serial dilution. Organs were stored in 3.5%PFA before histopathological sample preparation.

For inhibitor treatment, 5-6 weeks of C57BL/6J mice were infected by orally gavaging 10^7 CFU of STM WT. The inhibitor DFMO (Sigma, D193) was intraperitoneally injected every alternate day from day 1 at two doses 2mg/kg and 1mg/kg of body weight of mice. To study the colonisation in organs, the intestine (Peyer's patches), MLN, spleen and liver were isolated aseptically, 5 days post-infection, and the CFU was enumerated on differential and selective SS agar by serial dilution. For survival assay of mice 5-6 weeks old, C57BL/6J mice were infected by orally gavaging 10^8 CFU of STM WT. The inhibitor D, L-α-difluoromethylornithine (DFMO) was intraperitoneally injected every alternate day from day 1 at two doses 2mg/mice (125mg/kg of body weight) and

1mg/mice (62.5mg/kg of body weight). The doses were chosen and modified depending on previous studies on the treatment of tumours in mice (24, 25). However, the dose here in the case of infection scenario, has been reduced to two doses, 2mg/mice and 1mg/mice. The survival was monitored for 10 days. Likewise, organs were stored in 3.5% PFA before histopathological sample preparation.

For disease scoring, a small part of the liver was removed and fixed in 3.5% PFA. The 5 µm thick sections from fixed and paraffin-embedded tissues were cut onto glass slides and stained with haematoxylin and eosin (H&E) for histopathological examination. The comparison of pathological changes in the tissues was evaluated under light microscopy by a veterinary pathologist and scored with a scientific method using Mitchison's virulence/ pathology scoring system with some modifications, considering the aggregations of inflammatory cells, vascular congestion, and necrosis (26). The histopathology/ disease scores were graded as 0-3: 0 for normal pathology, 1 for mild/ minor pathology, 2 for moderate pathology, and 3 for severe pathological changes.

All experiments are done as per the norms of IEAC of the Indian Institute of Science, Bangalore. The approved protocol number is CAF/Ethics/852/2021.

Mass Spectrometry to determine intracellular GS-sp levels

The bacterial strains were grown in LB media with added 1mM hydrogen peroxide until the log phase of growth. The cells were centrifuged to remove the media, and the cells were resuspended in the lysis buffer (Sodium chloride, Tris, EDTA, 10% protease inhibitor cocktail) after washing with 1XPBS. The cells were lysed using sonication and centrifuged at 4°C to collect the cell lysate. Protein was precipitated using ice-cold acetone (Sigma, MS grade), 4 times the volume of the cell lysate, and by incubating at -20 °C overnight. The precipitated proteins were removed by

centrifugation, and the supernatant was used for analysis. Samples were analysed by ESI MS Q-TOF, impact HD (Bruker Daltonics Germany), and connected to Agilent HPLC 1260. Samples were passed through Agilent C18, 4.6X150mm column. The mobile phase used was water and acetonitrile with 0.1% formic acid. A linear gradient was used with a flow rate of 0.2ml/min. Data was analysed using Bruker Daltonics software Data analysis 4.1. Mass of GS-sp (Glutathionyl spermidine) is 434g/mol, and $(GS\text{-}sp)_2$ (oxidized form, Di-glutathionyl spermidine) is 866g/mol.

Results

Loss of spermidine transporter and biosynthesis genes in *Salmonella* Typhimurium compromises its ability to be phagocytosed by the macrophages

The pathoadaptation in *Salmonella* involves multiple players, which counteracts the stressful condition it encounters in the host macrophages. Polyamines are a group of well-studied stress response molecules, and we were interested in determining the expression of the spermidine transporter and biosynthesis genes in *Salmonella* Typhimurium. Here, we assessed the mRNA levels of *potA, potB, potC* and *potD* in STM WT upon infection into the RAW264.7 macrophage cell line. We noted that all the genes showed a 1.5-2 fold upregulation post 6 hours of infection into macrophages till 16 hours (**Fig 1 A)**. Further, our results showed that the spermidine biosynthesis enzymes *speE* and *speD* were upregulated 1.5 to 2 folds, post 6 hours to 16 hours post-infection into macrophages (**Fig 1 B)**. These results indicate that *Salmonella* Typhimurium enhances its intracellular spermidine biosynthesis and imports from the extracellular milieu. It might be a strategy of the pathogen to increase the intracellular pool of stress response molecules like the polyamine spermidine, as it encounters the hostile environment of host macrophages.

We then determined how the spermidine transporter and biosynthesis mutants (STM Δ*potCD*, STM Δ*speED* and STM Δ*potCD*Δ*speED*) behave upon infection into RAW264.7 macrophages. We infected STM WT, STM Δ*potCD*, STM Δ*speED* and STM Δ*potCD*Δ*speED* into RAW264.7 cells and observed that STM Δ*potCD*, STM Δ*speED* and STM Δ*potCD*Δ*speED* showed reduced phagocytosis by the macrophages compared to the wild type (**Fig 1 C)**. Interestingly, STM Δ*potCD*, STM Δ*speED* and STM Δ*potCD*Δ*speED* showed a compromised ability to proliferate intracellularly in the RAW264.7 cells, further validating a previous study (12)(**Fig S1 A)**. To further validate our results, we assessed the behaviour of the spermidine transporter and biosynthesis gene mutants in primary macrophages isolated from the peritoneal lavage of C57BL/6 mice. Likewise, the mutants showed attenuated proliferation and uptake by phagocytosis into the peritoneal macrophages (**Fig 1 D and S1 B)**. These results suggest that spermidine is a critical molecule in *Salmonella* Typhimurium to infect and survive in macrophages. To further investigate the reason behind the reduced ability to be taken up by macrophages upon loss of spermidine biosynthesis and transport, we treated STM WT, STM Δ*potCD*, STM Δ*speED* and STM Δ*potCD*Δ*speED* with mouse complement-sera. Upon pre-treatment with mouse complement-sera, we noted a rescue in the reduced uptake of the mutants by peritoneal macrophages isolated from C57BL/6 mice (**Fig 1 E)**. A study on *Salmonella* Typhimurium revealed that the non-flagellate and non-motile *Salmonella* show reduced phagocytosis by macrophages. The authors explained that non-flagellate and non-motile *Salmonella* collide less frequently with macrophages and get less time to maintain contact with the macrophage surface, thereby showing decreased phagocytosis (27). Our group previously showed that loss of spermidine production and import in *Salmonella* Typhimurium results in the loss of flagella formation on the bacterial cell surface(14). Thus, we determined the percentage phagocytosis for a flagellin-deficient strain of *Salmonella*

Typhimurium, STM Δ*fliC* and observed that STM Δ*potCD*, STM Δ*speED*, STM Δ*potCD*Δ*speE,* and STM Δ*fliC* similarly exhibited a significantly decreased ability to be taken up by the RAW264.7 macrophages (**Fig 1 F**). Furthermore, we observed a rescue of the attenuated percentage phagocytosis and fold proliferation of only STM Δ*speED* upon supplementation of spermidine (100μM) during the *in vitro* growth of bacteria prior to infection (**Fig 1 G and S1C**). We generated single gene mutants for abrogating the spermidine transport (STM Δ*potA*) and spermidine biosynthesis (STM Δ*speE*) function and further complemented the genes through a vector (STM Δ*potA: potA* and STM Δ*speE:speE*); we observed a recovery of the fold proliferation and percentage phagocytosis nearly to STM WT in the complemented strains (**Fig S1 D-E)**. Hence, the plausible explanation is that the reduced ability to form flagella in the spermidine mutants causes less frequent interaction with the macrophages and provides minimal contact time for infection, leading to reduced phagocytosis by the macrophages.

Figure 1: Loss of spermidine transporter and biosynthesis genes in *Salmonella* Typhimurium compromises its ability to be phagocytosed by the macrophages

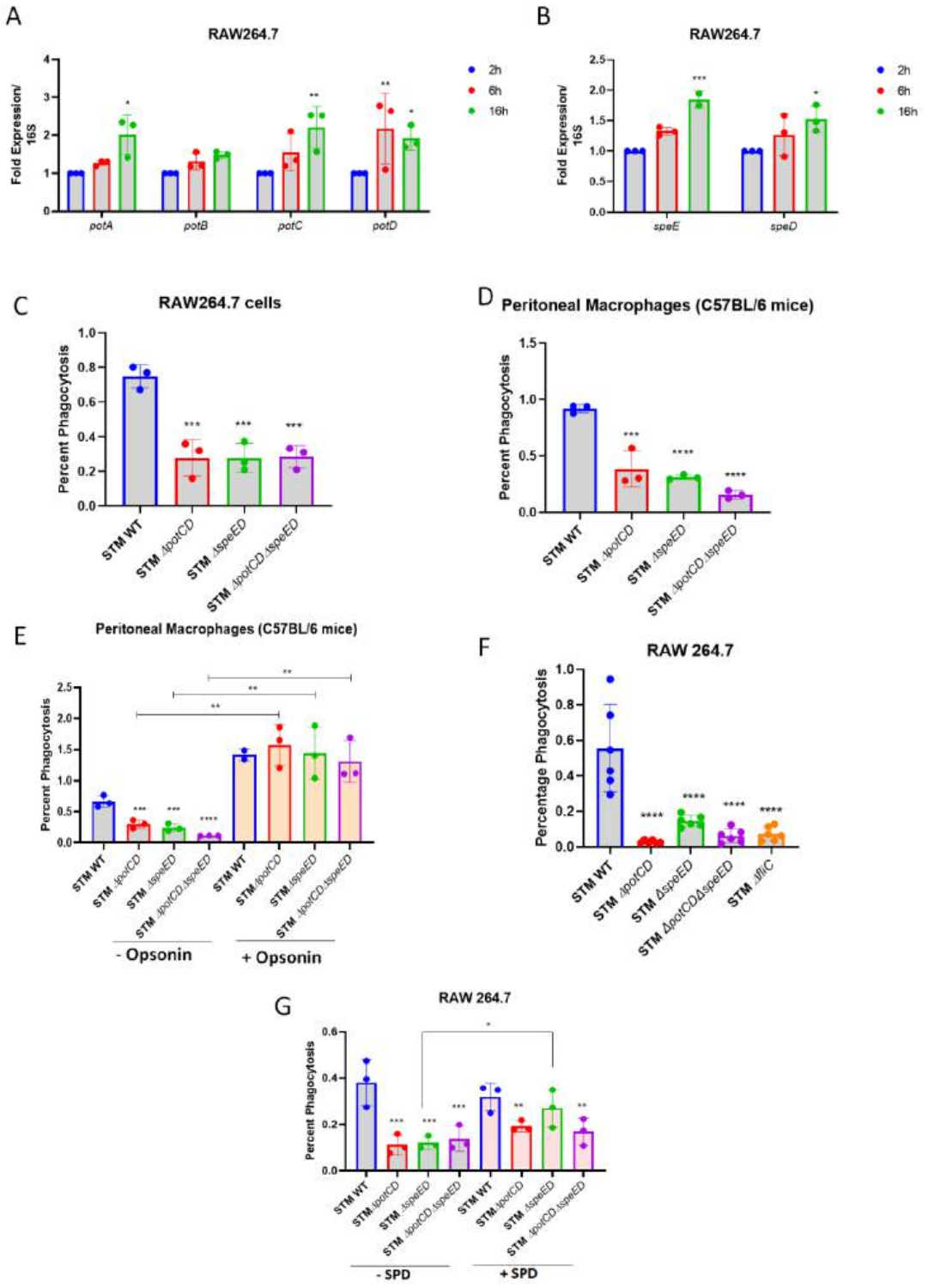

Figure 1: Loss of spermidine transporter and biosynthesis genes in *Salmonella* Typhimurium compromises its ability to be phagocytosed by the macrophages

A. The mRNA expression of spermidine transporter genes *potA, potB, potC* and *potD* in STM WT upon infection into RAW264.7 cells, B. The mRNA expression of spermidine biosynthesis genes *speE* and *speD* in STM WT upon infection into RAW264.7 cells, C. The percentage phagocytosis of the spermidine mutants in RAW264.7 cells, D. The percentage phagocytosis in primary macrophages isolated from peritoneal lavage of C57BL/6 mice, E. The percentage of phagocytosis upon pre-treatment with mouse-complement sera, which act as an opsonin, F. The percentage phagocytosis in RAW264.7 cells with flagellin mutant (STM *ΔfliC*) (data is from one experiment representative of 3 independent experiments), G. The percentage phagocytosis in RAW264.7 cells with the spermidine mutants grown in media supplemented with 100μM spermidine (SPD). One-way ANOVA with Dunnet's post-hoc test was used to analyze the data; p values ****<0.0001, ***<0.001, **<0.01, *<0.05. Two-way ANOVA with Tukey's post-hoc test was used to analyze the grouped data; p values ****<0.0001, ***<0.001, **<0.01, *<0.05. All data are represented as mean ±SD from three independent experiments (N=3)

Spermidine provides stress resistance in *Salmonella* Typhimurium by regulating the expression of numerous antioxidative enzymes

The loss of spermidine transport and biosynthesis function in *Salmonella* Typhimurium renders it incapable of proliferation and survival in macrophages. In the host macrophages, the bacteria encounter numerous threats, the foremost of which is the rapid oxidative burst mediated by NOX2. The reactive oxygen species superoxide radical can easily diffuse through the bacterial membrane

and pose a major threat to the pathogen. ROS acts on multiple molecules such as nucleic acids, proteins and lipids, thus damaging the cell membranes, DNA and proteins within the bacteria (28). Spermidine has been linked to stress response against oxidative stress and protects bacteria in *E. coli* and *Pseudomonas aeruginosa.* Thus, we were intrigued to understand the role of spermidine in antioxidative response in *Salmonella* Typhimurium. We examined the survival of STM WT, STM Δ*potCD*, STM Δ*speED*, and STM Δ*potCD*Δ*speE* upon exposure to the oxidative agent hydrogen peroxide *in vitro.* We noticed that at high concentrations of hydrogen peroxide, 5mM and 10mM, the STM Δ*potCD*, STM Δ*speED* and STM Δ*potCD*Δ*speE* showed significantly lesser survival than STM WT (**Fig 2 A**). Moreover, the complemented strains for spermidine transport and synthesis mutants showed a rescue in attenuated survival in the presence of high concentrations of hydrogen peroxide *in vitro* (**Fig S2 A)**. We further determined the expression of *potA, potB, potC, potD*, *speE* and *speD* in STM WT upon exposure to 1mM hydrogen peroxide. There was a 2-3 fold upregulation in the mRNA expression of the transporter genes over the untreated during the early log phase of growth (6 hours) and the late log phase of growth (12 hours) *in vitro* (**Fig S2 B-E**). Similarly, the biosynthesis genes *speE* and *speD* were 4-6 fold upregulated in their corresponding mRNA expressions during their early log phase of growth (6 hours) and the late log phase of growth (12 hours) *in vitro* (**Fig S2 F and G**). Our results show that *Salmonella* Typhimurium upregulates spermidine transport and biosynthesis upon oxidative stress, suggesting that spermidine mounts a protective function to aid bacterial survival in such a stressful condition.

Bacteria sense the environmental changes and cues to respond and adapt to the altered environment. They use the two-component systems, transcriptional activators and repressors, to alter gene expression in response to a stimulus (29). Polyamines in *E. coli* regulate multiple genes at the transcription and translation together, referred to as the "Polyamine modulon". These involve

the numerous mRNAs, tRNAs, sigma factors, translational factors, and two-component systems during bacterial growth and in stress conditions (30-32). *Salmonella* harbours multiple antioxidative enzymes to detoxify the ROS intracellularly (33). Our study so far shows that STM Δ*potCD*, STM Δ*speED,* and STM Δ*potCD*Δ*speE* are attenuated in survival under *in vitro* oxidative stress more than STM WT. To gain mechanistic insight into the attenuated survival of *Salmonella* Typhimurium, we determined the mRNA expression of the critical transcription factor *rpoS*, which activates the expression of the catalase enzymes (*katG and katE*) to detoxify hydrogen peroxide to water in the bacteria enzymatically (34). In both STM Δ*potCD* and STM Δ*speED,* the mRNA expression of *rpoS* is significantly downregulated from 6 hours post-infection in RAW264.7 cells (**Fig 2 B and C, S3 A**). Further, its downstream target *katG* was also downregulated in STM Δ*potCD* and STM Δ*speED* 6 hours post-infection into RAW264.7 cells (**Fig 2 D and E, S3 B**). We further assessed the mRNA expression of the transcription factor *soxR*, which regulates the expression of superoxide dismutases (*sodA* and *sodB*) (35). Upon infection in RAW264.7 cells, expression of *soxR* was significantly downregulated in STM Δ*potCD* and STM Δ*speED* with respect to STM WT (**Fig 2 F and G, S3 C**). Superoxide dismutases act on superoxide radicals, the potent ROS encountered in macrophages, converting to hydrogen peroxide. The mRNA expression of both *sodA* and *sodB* were downregulated in STM Δ*potCD* and STM Δ*speED* upon infection into RAW264.7 macrophages (**Fig 2 H-K, S3 D and E**). A significant antioxidant in most living organisms is glutathione (GSH), which directly acts as a quencher of ROS (36). GSH is synthesized by Glutathione synthase (GshA), which is regulated by EmrR transcription factor. We observed that the mRNA expression of *emrR* is downregulated in STM Δ*potCD* and STM Δ*speED* upon infection into RAW264.7 macrophages (**Fig 2 L and M, S3 F**). Similarly, *gshA* transcript expression is downregulated (**Fig 2 N and O, S3 G)**. To further validate the down regulation of

the glutathione synthesis arm in spermidine transport and biosynthesis mutants, we determined the intracellular GSH levels and noted that in STM Δ*potCD,* STM Δ*speED* and STM Δ*potCD*Δ*speED* the levels were significantly less (**Fig S3H and I).** Taken together, these results indicate that spermidine regulates the transcription of multiple transcription factors involved in oxidative stress response in *Salmonella* Typhimurium. Importantly, we found a mechanism of oxidative stress resistance in *Salmonella* Typhimurium regulated by spermidine, potentiating the survival of the bacteria.

Figure 2: Spermidine provides stress resistance in *Salmonella* Typhimurium by regulation of the expression of numerous antioxidative enzymes

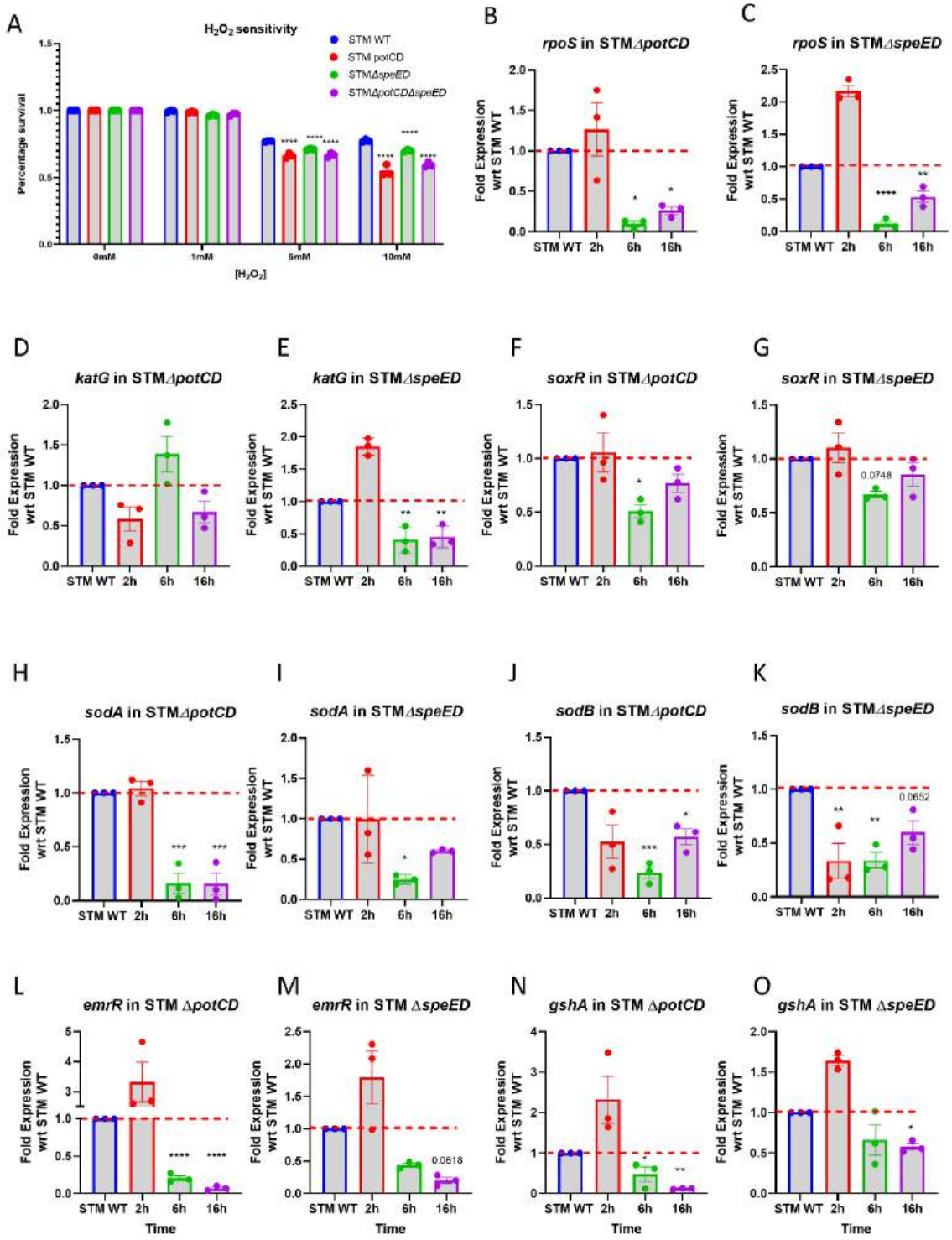

Figure 2: Spermidine provides stress resistance in *Salmonella* Typhimurium by regulation of the expression of numerous antioxidative enzymes

A. The *in vitro* hydrogen peroxide sensitivity assay with the spermidine transport and biosynthesis mutants ((data is from one experiment representative of 3 independent experiments)), B. The mRNA expression of stress-responsive transcription factor *rpoS* in STM *ΔpotCD* upon infection into RAW264.7 cells, C. The mRNA expression of stress-responsive transcription factor *rpoS* in STM *Δwas speED* upon infection into RAW264.7 cells, D. The mRNA expression of *katG* in STM *ΔpotCD* was upon infection into RAW264.7 cells, E. The mRNA expression of *katG* in STM *ΔspeED* upon infection into RAW264.7 cells, F. The mRNA expression of oxidative stress-responsive transcription factor *soxR* in STM *ΔpotCD* upon infection into RAW264.7 cells, G. The mRNA expression of oxidative stress-responsive transcription factor *soxR* in STM *ΔspeED* upon infection into RAW264.7 cells, H. The mRNA expression of *sodA* in STM *ΔpotCD* upon infection into RAW264.7 cells, I. The mRNA expression of *sodA* in STM *ΔspeED* upon infection into RAW264.7 cells, J. The mRNA expression of *sodB* in STM *ΔpotCD* upon infection into RAW264.7 cells, K. The mRNA expression of *sodB* in STM *ΔspeED* upon infection into RAW264.7 cells, L. The mRNA expression of glutathione synthetase specific transcription factor *emrR* in STM *ΔpotCD* upon infection into RAW264.7 cells, M. The mRNA expression of glutathione synthetase-specific transcription factor *emrR* in STM *Δwas speED* upon infection into RAW264.7 cells, N. The mRNA expression of *gshA* in STM *ΔpotCD* upon infection into RAW264.7 cells, O. The mRNA expression of *gshA* in STM *ΔspeED* upon infection into RAW264.7 cells. One-way ANOVA with Dunnet's post-hoc test was used to analyse the data, p

values****<0.0001, ***<0.001, **<0.01, *<0.05. All data are represented as mean±SD from three independent experiments (N≥3).

Spermidine controls a novel enzyme Glutathionyl-spermidine synthetase in *Salmonella* Typhimurium, and together mount an intracellular antioxidative response

The spermidine synthesized from putrescine has two fates. It is either acetylated by the enzyme SpeG or covalently conjugated to GSH to form Glutathionyl-spermidine (GS-sp) catalysed by Glutathionyl-spermidine synthetase (Gss). Tabor (1974) first discovered the existence of this enzyme in *E. coli* (37). In *E. coli* GS-sp is generated at a higher level in the stationary phase and very less in the late exponential phase. It also interacts and modifies the thiol-containing proteins under high H_2O_2-containing media, forming Gsp-thiolated proteins (PS-Gsp). Certain *in vitro* experiments with dehydro-ascorbate suggested that GS-sp might have higher antioxidant properties than GSH (38) and may be more effective in protecting against DNA damage by free radicals (39). However, in *E. coli,* Gss could not be linked to its pathogenicity (40). Among *Enterobacteriaceae*, *Salmonella* was found to possess this unique enzyme. Our *in silico* analysis suggested that the enzyme in *Salmonella* Typhimurium (GspSA, encoded by *gsp*) has 90% identity with *E. coli gss,* and the SWISS-MODEL predicts it to be a homo-dimeric protein (**Fig S4 A-C**). Also, the spermidine synthesised by SpeE in *Salmonella* Typhimurium is directly fed into the pathway to synthesise GS-sp. Thus, we investigated this novel enzyme's biological role in *Salmonella* Typhimurium. We noted that the mRNA expression of *gsp* is significantly upregulated at the late-log phase of growth of STM WT in LB media in the presence of H_2O_2 (**Fig S4 D**). Upon infection into RAW264.7 cells, STM WT upregulates the mRNA expression of *gsp* at 6 hours and 16 hours post-infection into RAW264.7 cells (**Fig 3 A**). Further, the *Salmonella* Typhimurium

mutant of *gsp* (STM Δ*gsp*) showed attenuated proliferation in RAW264.7 cells similar to STM Δ*katG,* which has reduced capability to detoxify ROS, while upon complementation of *gsp* in the mutant (STM Δ*gsp:gsp*) partially rescues the phenotype and we observe a higher fold proliferation than the mutant (**Fig 3 B)**. Thus, our results suggest that *gsp* is important in *Salmonella* Typhimurium to survive and cope with the oxidative stress and hostile environment of macrophages. Interestingly, the mRNA expression of *gsp* was downregulated in both STM Δ*potCD* and STM Δ*speED* at 16 hours post-infection into RAW264.7 macrophages (**Fig 3 C and D)**. These findings show that spermidine regulates GspSA enzyme and thereby controls the flux of spermidine into the GspSA pathway. Also, it further potentiates the ability of *Salmonella* Typhimurium to mount an antioxidative response by regulating *gsp* expression.

GspSA enzyme in Trypanosomes was named Trypanothione synthetase, while the conjugate is called Trypanothione (TSH). In trypanosomes, TSH is essential, and these organisms rely entirely on TSH and possess no GSH reductase. Also, they have evolved to use TSH reductase instead of GSH reductase, Glutaredoxins or Thioredoxins (41). In *E. coli* GS-sp forms bonds with the Cysteine thiol groups of numerous proteins and protect them from oxidation under oxidative stress. Cysteine thiol groups are highly prone to attack by ROS and get oxidized to sulphinic and sulphonic acids. In *Salmonella* Typhimurium, we observe that loss of *gsp* results in attenuated proliferation and survival in macrophages. Thus, we investigated the survival of STM Δ*gsp* upon exposure to hydrogen peroxide *in vitro*. STM Δ*gsp* exhibited reduced survival in high 5mM and 10mM concentrations of H_2O_2 (**Fig S4 E**). Likewise, upon exposure to agents of oxidative stress and nitrosative stress H_2O_2 and $NaNO_2$ together, we observe that STM Δ*gsp* exhibited reduced survival at higher concentrations such as 5mM and 10mM compared to STM WT (**Fig 4 E**). Thus, *gsp* is critical in *Salmonella* Typhimurium to shield the bacteria from the action of ROS and RNS.

As we observed, spermidine transporter and biosynthesis mutants and *gsp* mutants of *Salmonella* Typhimurium are compromised in their survival under oxidative stress and in macrophages; thus, we were interested in assessing the intracellular ROS detoxification abilities of the strains. We determined the intracellular ROS in STM WT, STM Δ*potCD*, STM Δ*speED*, STM Δ*potCD*Δ*speE,* STM Δ*gsp* and STM Δ*katG*. Interestingly, STM Δ*potCD*, STM Δ*speED*, STM Δ*potCD*Δ*speE,* STM Δ*gsp* and STM Δ*katG* showed significantly higher intracellular ROS levels when they were exposed to 5mM and 10mM H_2O_2 (**Fig 3 F**). Further, the complemented strains for spermidine transport and synthesis mutants showed reduced intracellular ROS in the presence of high concentrations of hydrogen peroxide *in vitro* (**Fig S4 F)**. These results suggest that lower intracellular levels of spermidine correlate to higher intracellular ROS levels in *Salmonella* Typhimurium. To validate our observed results, we utilised a genetically engineered tool to sense the redox status of the bacterial cytosol. We used pQE60-Grx1-roGFP2 plasmid that contains roGFP2, a genetically modified form of GFP. The glutaredoxin (Grx1) fused to the roGFP2 reversibly transfers electrons between the cytosolic pool of GSH/GSSG and the thiol group of roGFP2, and the ratio of fluorescence ratio at 408nm and 488nm determine the redox status of bacterial cytoplasm (22). We observed that STM Δ*potCD*, STM Δ*speED* harbouring the pQE60-Grx1-roGFP2 showed a higher ratio of 405nm/488nm compared to STM WT in the presence of 5mM H_2O_2 *in vitro* and upon infection into RAW 264.7 macrophages (**Fig 3 G and H**). However, STM Δ*gsp* did not show a significantly higher 408nm/488nm ratio. Moreover, upon supplementation of the growth media with 100 μM spermidine, only in STM Δ*speED* we observed a lower intracellular ROS and lesser 408nm/488nm in higher concentrations of H_2O_2 (**Fig S4 G and H)**. Thus, our results indicate that spermidine is critical in mounting an antioxidative response to detoxify the intracellular ROS by regulating multiple antioxidant genes in *Salmonella*

Typhimurium. To validate our observed results, we used mass spectrometry to determine the intracellular levels of glutathionyl-spermidine (Gs-sp) in STM WT, STM Δ*potCD*, STM Δ*speED* and STM Δ*gsp*. Our study qualitatively shows that the synthesis of GS-sp and $(GS\text{-}sp)_2$ (oxidized form, di-glutathionyl-spermidine) in STM WT upon exposure to 1mM hydrogen peroxide, which is absent in the spermidine mutants and STM Δ*gsp* (**Fig S5 A and B**). We further determined the presence of PS-Gsp and showed that STM WT modifies proteins by GS-sp (detected by anti-spermidine antibody), which is reduced upon treatment with beta-mercaptoethanol. The spermidine mutants show less modification, which is almost negligible in STM Δ*gsp* (**Fig S5 C-E**).

We observe that STM Δ*potCD* STM Δ*speED* shows a higher intracellular ROS than STM Δ*gsp.* Thus, to understand does STM Δ*gsp* phenocopy STM Δ*potCD* STM Δ*speED*, we generated double mutants STM Δ*gsp*Δ*potCD* and STM Δ*gsp*Δ*speED.* We find that the double mutants show a similar reduced fold proliferation and percentage phagocytosis in RAW 264.7 cells (**Fig S6 A-B)**. However, they show an enhanced intracellular ROS upon exposure to hydrogen peroxide (**Fig S6 C)**. Upon co-infection of the double mutants with STM Δ*gsp* in C57BL/6 mice, we see that STM Δ*gsp* competes with the double mutants in colonizing the liver (**Fig S6 D-E)**. To further dissect the role of spermidine in the protection of *Salmonella* Typhimurium from oxidative stress, we infected STM WT, STM Δ*potCD*, STM Δ*speED*, STM Δ*potCD*Δ*speE,* STM Δ*gsp* and STM Δ*katG* in primary macrophages isolated from the peritoneal lavage of *gp91phox -/-* mice. Gp91Phox is the major subunit of the NOX2 complex that aids in the catalysis of oxygen to superoxide radicals. Interestingly, we observe a rescue in the attenuated fold proliferation of STM Δ*potCD*, STM Δ*speED*, STM Δ*potCD*Δ*speE,* STM Δ*gsp* and STM Δ*katG* in peritoneal macrophages isolated

from *gp91phox -/-* mice (**Fig 3 I**). Our results demonstrate the vital role of spermidine in oxidative stress resistance in *Salmonella* Typhimurium.

Figure 3: Spermidine controls a novel enzyme Glutathionyl-spermidine synthetase in *Salmonella* Typhimurium, and together mount an intracellular antioxidative response

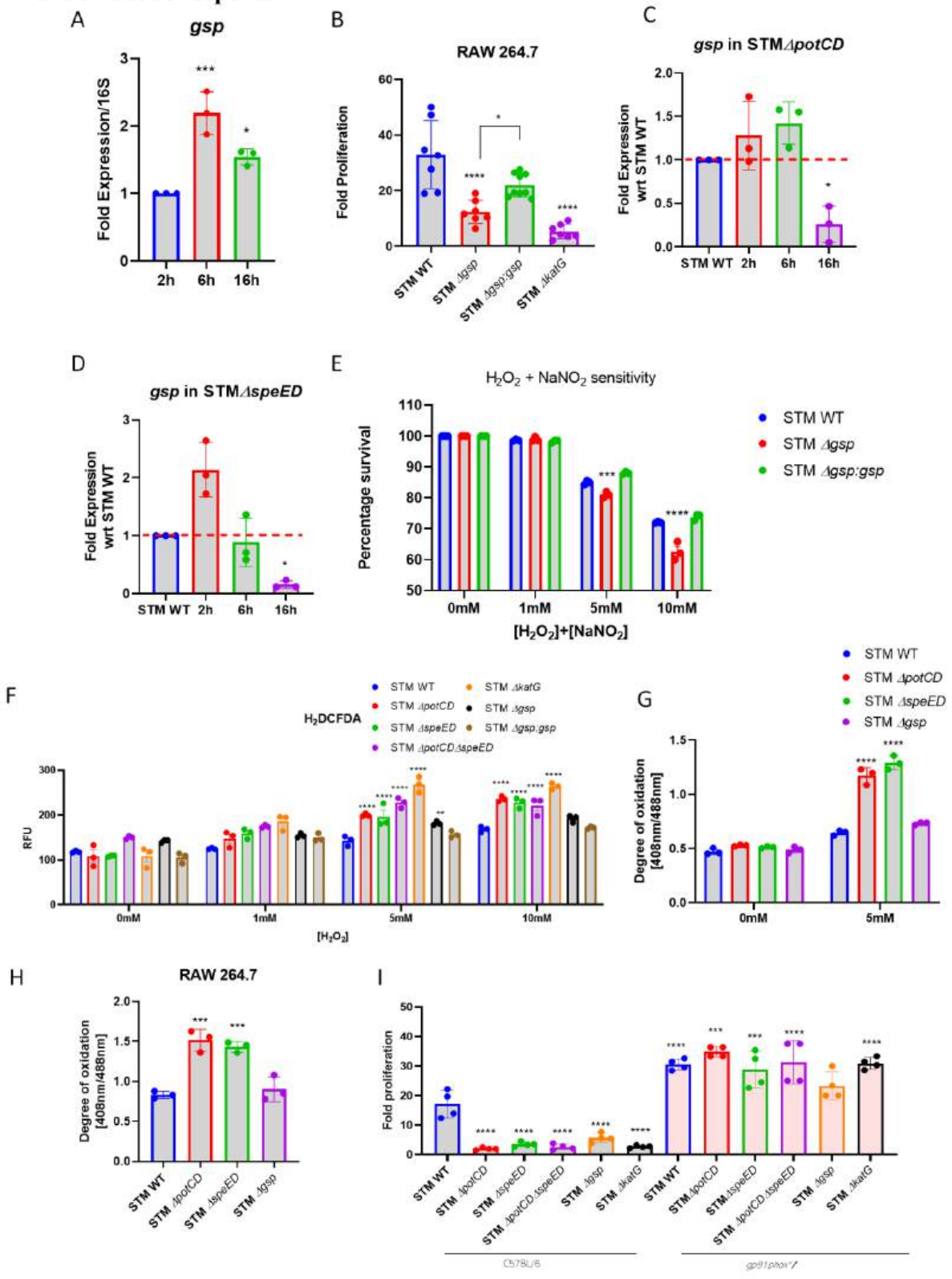

Figure 3: Spermidine controls a novel enzyme Glutathionyl-spermidine synthetase in *Salmonella* Typhimurium, and together mount an intracellular antioxidative response

A.The mRNA expression of *gsp* in STM WT upon infection into RAW264.7 cells, B The fold proliferation of STM WT, STM *Δgsp* and STM *Δgsp:gsp* in RAW264.7 cells, (data is from one experiment representative of 3 independent experiments) C. The mRNA expression of *gsp* in STM *ΔpotCD* upon infection into RAW264.7 cells, D. The mRNA expression of *gsp* in STM *ΔspeED* upon infection into RAW264.7 cells, E The *in vitro* Hydrogen peroxide and nitric oxide sensitivity assay (data is from one experiment representative of 3 independent experiments), F. Intracellular reactive oxygen species determination using the cell-permeable H_2DCFDA dye, G. The intracellular degree of oxidation in spermidine and *gsp* mutants using pQE60-grx1-roGFP2 construct *in vitro*, H. The intracellular degree of oxidation using pQE60-grx1-roGFP2 construct in spermidine and *gsp* mutants upon infection into RAW 264.7 cells, I. The fold proliferation in primary macrophages isolated from wild-type C57Bl/6 mice and *gp91phox-/-* mice (data is from one experiment representative of 3 independent experiments). One-way ANOVA with Dunnet's post-hoc test was used to analyze the data; p values ****<0.0001, ***<0.001, **<0.01, *<0.05. Two-way ANOVA with Tukey's post-hoc test was used to analyze the grouped data; p values ****<0.0001, ***<0.001, **<0.01, *<0.05. All data are represented as mean±SD from three independent experiments (N≥3).

Spermidine is critical for *Salmonella* Typhimurium to colonise the primary and secondary sites of infection in mice

Salmonella infects the host and breaches the epithelial cells at the Peyer's patches in the distal ileum, it disseminates to the secondary sites of infection, namely the Mesenteric Lymph node (MLN), spleen and liver. *Salmonella* is taken from the basolateral surface of the epithelial cells at the lamina propria by the macrophages and polymorphonuclear cells (PMN). We observed that the spermidine transporter and biosynthesis mutants show attenuated survival in macrophages and under oxidative stress *in vitro.* We were intrigued to study the behaviour of the mutants during *in vivo* colonisation in the mouse model of *Salmonella* infection. We infected C57BL/6J mice by orally gavaging with STM WT, STM Δ*potCD*, STM Δ*speED*, STM Δ*potCD*Δ*speE,* STM Δ*gsp* and STM Δ*katG* at a CFU of 10^7 per mouse. We noted that STM Δ*potCD*, STM Δ*speED*, STM Δ*potCD*Δ*speE,* and STM Δ*katG* showed a significantly lower organ burden in Peyer's patches, MLN, spleen, and liver upon oral gavage **(Fig 4 A-E)**. Meanwhile, STM Δ*gsp* shows significantly lower colonization compared to STM WT in MLN and liver upon oral gavage (**Fig 4 A-E)**. Our previous study showed that the spermidine transporter and biosynthesis mutants exhibit poor invasiveness into IECs, which can explain our *in vivo* colonisation upon oral gavage (13). Oral gavage mimics the physiological route of *Salmonella* infection into its host. Hence, it requires to be able to breach the intestinal barrier successfully. Incapability to invade the IECs in STM Δ*potCD*, STM Δ*speED*, STM Δ*potCD*Δ*speE* and STM Δ*gsp* explains the diminished colonisation in the organs. To dissect the role of spermidine in the *in vivo* colonisation, we infected C57Bl/6J mice intraperitoneally by bypassing the entry and breaching the epithelial barrier. We observed that upon infecting intraperitoneally, STM Δ*speED*, STM Δ*potCD*Δ*speE,* STM Δ*gsp* and STM Δ*katG* exhibited reduced colonisation in the spleen and liver and less dissemination in blood compared to STM WT (**Fig 4 F-I)**. Meanwhile, STM Δ*potCD* was found to colonise less in the liver and showed less dissemination in blood upon intraperitoneal injection (**Fig 4 F-I)**. Also, the

histopathological sections show significantly less liver tissue damage with STM Δ*potCD*, STM Δ*speED*, STM Δ*potCD*Δ*speE,* STM Δ*gsp* and STM Δ*katG*, which is validated by disease scoring of the same (**Fig 4 J and K, S7 A-G)**. Our results thus show that spermidine aids in the *in vivo* pathogenesis and virulence of *Salmonella* Typhimurium.

Figure 4: Spermidine is critical for *Salmonella* Typhimurium to colonise the primary and secondary sites of infection in mice

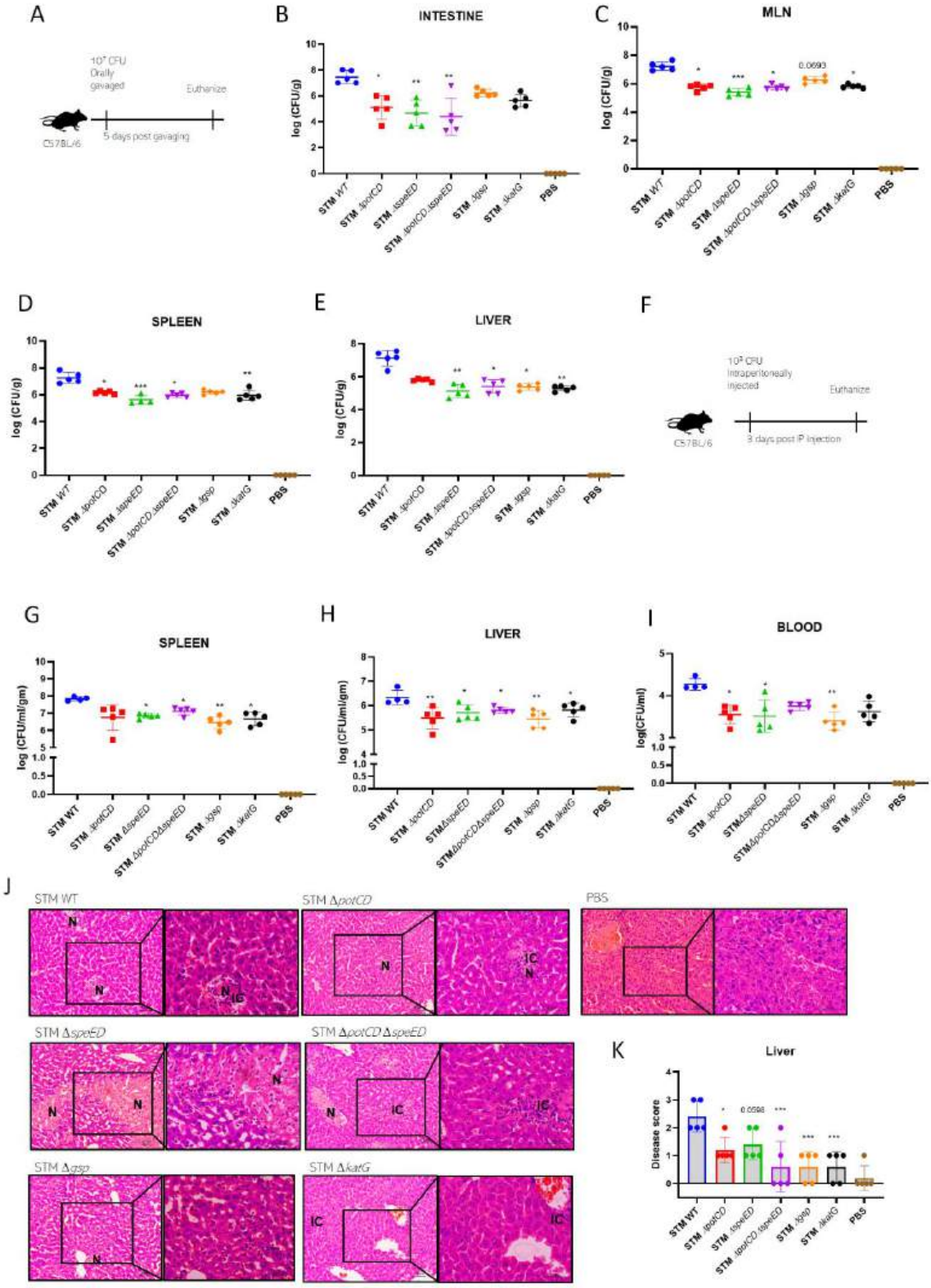

Figure 4: Spermidine is critical for *Salmonella* Typhimurium to colonise the primary and secondary sites of infection in mice

A. The experimental protocol for organ burden in C57BL/6 mice by orally gavaging 10^7 CFU per mice, B. The organ burden post 5 days of oral gavage in the intestine, C. in the Mesenteric lymph node (MLN), D. in the spleen, E. in the liver, F. The experimental protocol for organ burden in C57BL/6 mice upon intraperitoneal (I.P) infection with 10^3 CFU per mice, G. The organ burden 3 days post I.P infection in the spleen, H. in the liver, I. dissemination in blood, J. The hematoxylin and eosin staining of the sections of the liver 3 days post I.P infection of C57Bl/6 mice (N=5, scale bar- 50μM), K. Disease score from the histopathological sections of the liver. Here, (IC) Multiple aggregations of inflammatory cells dispersed in the liver parenchyma, (N) shows several small necrotic areas, (C) congestion and damage to the endothelial lining of the central vein, (HPV) congestion of the hepatic portal vein. The disease score is 0 for normal pathology, 1 for mild/ minor pathology, 2 for moderate pathology, and 3 for severe pathological changes. Non-parametric One-way ANOVA (Kruskal Wallis) with Dunn's post-hoc test was used to analyse organ burden in mice; p values ****<0.0001, ***<0.001, **<0.01, *<0.05. One-way ANOVA with Dunnet's post-hoc test was used to analyze the rest of the data; p values ****<0.0001, ***<0.001, **<0.01, *<0.05. All data are represented as mean±SD from three independent experiments (N≥3).

***Salmonella* rewires host polyamine metabolism to potentiate its survival within host macrophages**

Most of the intracellular pathogens establish their persistence in the phagocytic cells and are often found to be associated with different populations of macrophages. Like *Brucella abortus, it*

preferentially resides in the Alternatively activated macrophages (AAM), where it survives and replicates by exploiting the host polyamines. A research group has shown that the metabolism of AAM is shifted to increase polyamine biosynthesis by *Brucella abortus* and thereby promote bacterial survival (42). Similarly, *Salmonella* also resides in macrophages, a way to lead chronic infections. We were interested to know whether *Salmonella* exploits the host polyamines and leads to a rewiring of host cell metabolism. To understand the host-pathogen relationship in depth, we assessed the mRNA expression of Ornithine decarboxylase 1 (*mOdc,* mouse Ornithine decarboxylase), which catalyses the rate-determining step of polyamine biosynthesis and Spermidine synthase (*mSrm,* mouse Spermidine synthase) that synthesises spermidine from putrescine by transferring the aminopropyl group from decarboxylated-S-adenosyl methionine in RAW264.7 cells upon infection with STM WT. We observed that mRNA expression of *mOdc1* and *mSrm* were upregulated at 6- and 16-hours post-infection (**Fig 5 A and B**). Further, the mRNA expression of *mOdc1* and *mSrm* were enhanced in the spleen and liver of C57BL/6 mice 5 days post oral gavage with STM WT (**Fig C- F**). Our results show that *Salmonella* Typhimurium enhances the expression of host polyamine biosynthesis genes upon infection into the host. Moreover, we have previously observed that the *Salmonella* Typhimurium that cannot import spermidine cannot survive and proliferate as much as STM WT in macrophages. To delve further into the role of host-acquired polyamines, we knocked down *mOdc1* in RAW264.7 cells (**Fig S8 A**). Upon knockdown of *mOdc1*, *Salmonella* Typhimurium showed significantly attenuated proliferation in RAW264.7 cells (**Fig 5 G**). However, the knockdown of *mOdc1* did not alter the percentage of phagocytosis by the macrophages (**Fig S8 C)**. Similarly, we knocked down *Srm* in RAW264.7 cells and observed that the knockdown of spermidine synthase in the host compromises

the ability of STM WT to proliferate and get phagocytosed by the macrophages (**Fig S8 B, D and E)**.

The question that arises is how *Salmonella* regulates the host polyamine metabolic pathways. *Salmonella* utilizes pathogenicity island 1 and 2 (SPI-1 and SPI-2) encoded effectors to enter and survive in the specialized host niches (43, 44). Although SPI-1 is well studied in the initial process of invasion, recent studies suggest that both SPI-1 and SPI-2 effectors are required for SCV maturation and *Salmonella* survival in the host cells (45-47). Thus, to investigate how *Salmonella* modulates host cell polyamine metabolism, we infected RAW264.7 cells with an SPI-1 mutant (STM Δ*invC*) and a SPI-2 mutant (STM Δ*ssaV*), both of which cannot export effectors of SPI-1 and SPI-2 respectively. We observed that the mRNA expression of *mOdc1* and *mSrm*, were significantly downregulated in macrophages infected with STM Δ*invC* and STM Δ*ssaV* compared to in STM WT (all normalized to Uninfected) (We further determined the intracellular spermidine by immunofluorescence and found that macrophages infected with STM Δ*invC* and STM Δ*ssaV* showed reduced spermidine production compared to STM WT and uninfected cells (**Fig 5J and K, S8 F)**. Thus, our data suggests that *Salmonella* utilizes effectors from SPI-1 and SPI-2 to modulate the host cell polyamine metabolic pathways. Furthermore, a stronger effect was observed with STM Δ*invC* in regulating host polyamine metabolism.

Figure 5: *Salmonella* rewires host polyamine metabolism to potentiate its survival within host macrophages

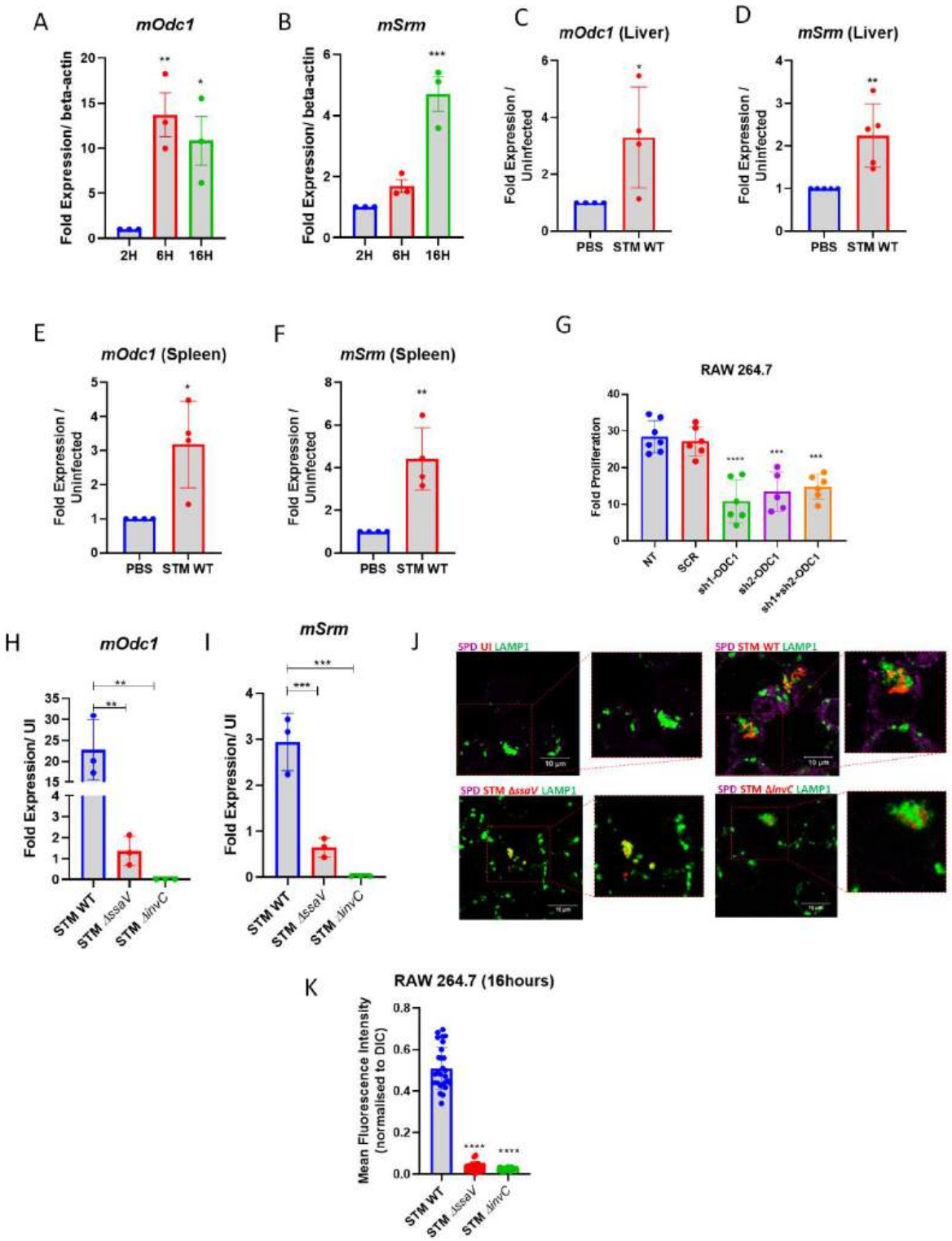

Figure 5: *Salmonella* rewires host polyamine metabolism to potentiate its survival within host macrophages

A. The mRNA expression of *mOdc1* (mouse ornithine decarboxylase) in RAW264.7 cells upon infection with STM WT, B. The mRNA expression of *mSrm* (mouse spermidine synthase) in RAW264.7 cells upon infection with STM WT, C. The mRNA expression of *mOdc1* (mouse ornithine decarboxylase) in the liver of C57BL/6 mice 5 days post-infection with STM WT by oral gavage, D. The mRNA expression of *mSrm* (mouse spermidine synthase) in the liver of C57BL/6 mice 5 days post-infection with STM WT by oral gavage, E. The mRNA expression of *mOdc1* (mouse ornithine decarboxylase) in the spleen of C57BL/6 mice 5 days post-infection with STM WT by oral gavage, F. The mRNA expression of *mSrm* (mouse spermidine synthase) in the spleen of C57BL/6 mice 5 days post-infection with STM WT by oral gavage, G. The fold proliferation of STM WT in RAW264.7 cells upon transient knockdown of *mOdc1,* (data is from one experiment representative of 3 independent experiments) H. The percentage phagocytosis of STM WT in RAW264.7 cells upon transient knockdown of *mOdc1.* Here, SCR is Scrambled (no target for knockdown), and two different targeted shRNA were used for knockdown purposes: Sh1 is shRNA-1 for knockdown, Sh2 is shRNA-2 for knockdown, and Sh1+Sh2 indicates where both the shRNAs were used to obtain the knockdown, NT is untransfected, H. The mRNA expression of *mOdc1* (mouse ornithine decarboxylase) in RAW264.7 cells upon infection with STM WT, STM Δ*ssaV,* and STM Δ*invC*, normalized to the expression in uninfected macrophages, I. The mRNA expression of *mSrm* (mouse spermidine synthase) in RAW264.7 cells upon infection with STM WT, STM Δ*ssaV,* and STM Δ*invC*, normalized to the expression in uninfected macrophages, J. Immunofluorescence imaging to study spermidine in RAW 264.7 cells upon infection with STM WT, STM Δ*invC,* STM Δ*ssaV,* K. The quantification of (J) (data is from one experiment

representative of 3 independent experiments). Here, green is Anti-mouse LAMP1(Alexa fluor 488), Red is pFPV-M-cherry expressing *Salmonella* strains, magenta is anti-Spermidine (Alexa fluor 647), and UI- uninfected. One-way ANOVA with Dunnet's post-hoc test was used to analyze the data; p values****<0.0001, ***<0.001, **<0.01, *<0.05. All data are represented as mean±SD from three independent experiments (N≥3).

The chemopreventive drug DFMO reduces *Salmonella* Typhimurium burden in the host by enhancing nitric oxide production

Polyamines are essential molecules in eukaryotes, with multiple roles in differentiation, proliferation, and development. Many studies have shown that polyamine levels are upregulated in cancer cells, and elevated levels of polyamines are associated with breast cancer, neuroblastoma, hepatocellular carcinoma, prostate cancer, lung cancer, colorectal cancer, and leukaemia (48-52). D, L-α-difluoromethylornithine (DFMO), an inhibitor of ODC, was developed as a potent drug to treat cancer in 1970 (53). DFMO irreversibly binds to the active site of ODC and acts as a suicide inhibitor, thereby reducing polyamine levels and having a cytostatic effect. It was effective only in neuroblastoma as a single therapeutic agent and clinical trials for other cancer types were unsatisfactory (54, 55). However, DFMO has been successfully developed as a chemopreventive drug, with FDA approval for treating Human African Trypanosomiasis (HAT) (56, 57). To test whether DFMO can be used as a therapeutic drug against *Salmonella* infection, we treated RAW264.7 cells with DFMO during the *Salmonella* Typhimurium infection. We observed a significant attenuation in the fold proliferation of STM WT (**Fig 6 A)**. Studies have shown that DFMO binds to ODC to prevent further putrescine production from ornithine, acts on Arginase1,

and reduces the available pool of ornithine for polyamine biosynthesis (58, 59). This ensures the arginine flux is fed into the nitric oxide synthase (NOS2) pathway and leads to elevated levels of nitric oxide in the cell (60). We assessed the mRNA expression of *mNos2* upon knockdown of *mOdc1* in RAW264.7 cells, followed by infection with STM. We observed an upregulation of *mNos2* mRNA levels at 6- and 16-hours and an upregulation of mNOS2 protein at 16 hours post-infection in RAW264.7 cells (**Fig 6 B S9 A and B)**. Further, we determined nitric oxide levels using a cell-permeable dye DAF_2DA and noted that upon treatment with DFMO there was higher production of nitric oxide (**Fig 6 C and D)**. While when we inhibited mNos2 using 1400W, the nitric oxide levels did not increase on further treatment of DFMO (**Fig S9 C and D)**. Furthermore, infecting primary macrophages isolated from *iNOS-/-* mice we observed that the fold proliferation is not altered upon treatment of DFMO from the untreated cells (**Fig 6 E, S9 E)**. Taken together, our results demonstrate the role of DFMO in diminishing the survival and proliferation of *Salmonella* Typhimurium by blocking Odc1 and enhancing nitric oxide production in murine macrophages.

To further address whether DFMO also acts as a potent anti-*Salmonella* drug in mice model of infection, we infected C57BL/6 mice with 10^7 CFU per mouse by oral gavage. Every alternate day, the mice were injected with DFMO in two different doses for two cohorts [2mg/mice (125mg/kg of body weight) and 1mg/mice (62.5mg/kg of body weight)]. Five days post oral gavage, we observed that DFMO treatment of 2mg/kg body weight of mice significantly reduced the colonisation of STM WT in the intestine, MLN, spleen and liver than in the untreated mice (**Fig 6 F-J)**. Further, using immunofluorescence, we observed that DFMO significantly reduced the colonisation of STM and the levels of spermidine in mouse ileum (**Fig S10 A-D).** Moreover, treatment of mice with DFMO at a dose of 2mg/mice increased the survival of mice upon infection

with STM WT (**Fig 6 K and L)**. Also, the weight reduction in mice treated with DFMO at a dose of 2mg/mice was less upon infection with STM WT (**Fig S10 E)**. Next, we evaluated the tissue damage upon infection of STM in mice liver. The results show that DFMO treatment of mice at a dose of 2mg/mice significantly lowered the disease score, suggesting lesser tissue damage than untreated (**Fig 6 M and N, S10 F)**. Thus, DFMO serves as a potential drug to treat *Salmonella* infection in mice by reducing the bacterial burden and tissue damage in mice and enhancing the survival of mice upon infection with STM.

Figure 6: The chemopreventive drug DFMO, reduces *Salmonella* Typhimurium burden in the host by enhancing nitric oxide production

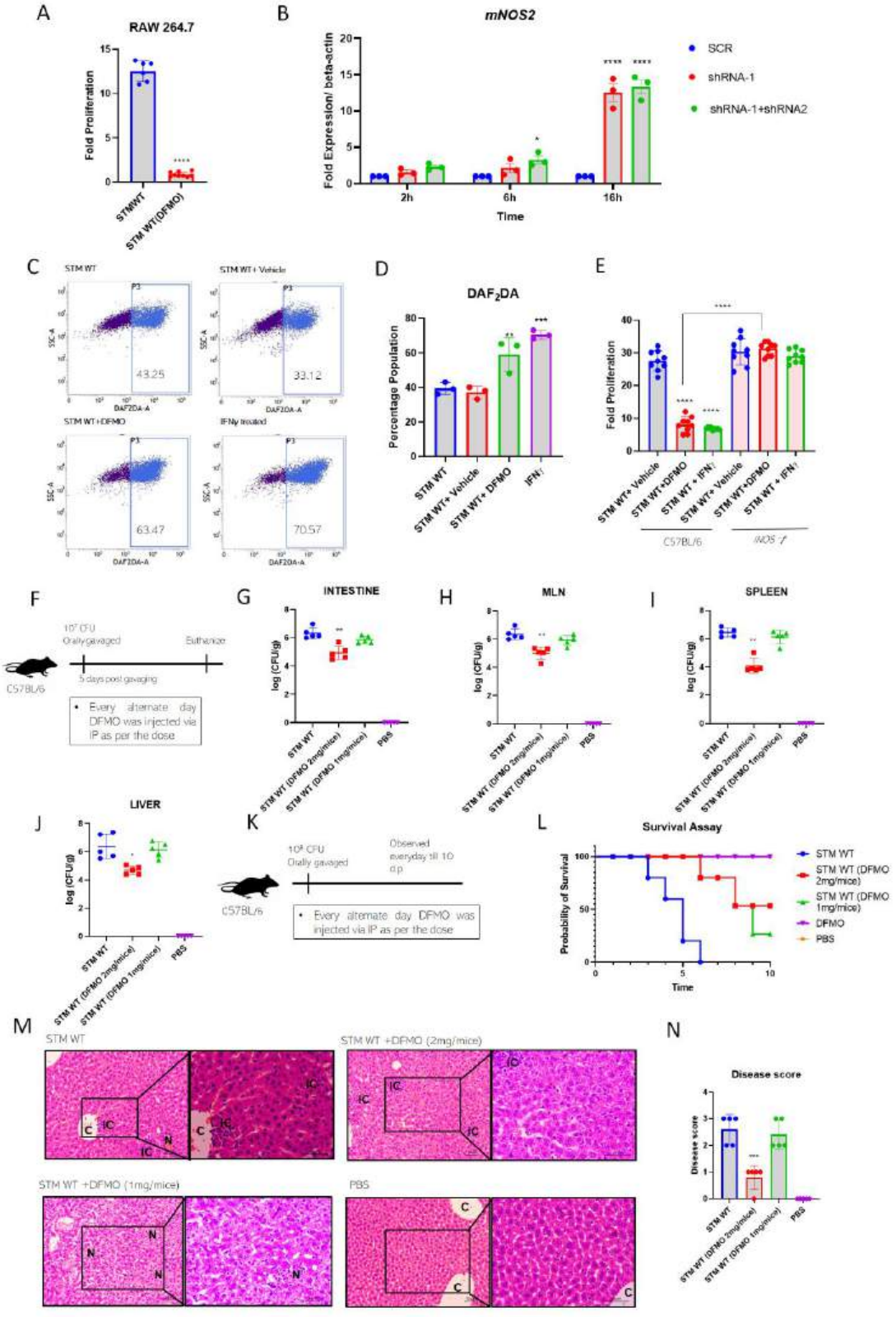

Figure 6: The chemopreventive drug DFMO reduces *Salmonella* Typhimurium burden in the host by enhancing nitric oxide production

A. The intracellular fold proliferation of STM WT in RAW264.7 cells upon treatment with Difluoromethyl ornithine (DFMO) (5μM), quantified by Gentamicin protection assay, B. The mRNA expression of *mNos2*(mouse Nitric oxide synthase) in RAW264.7 cells, upon transient knockdown of *Odc1* followed by infection with STM WT, is normalized to beta-actin as an internal control, C. The representative scatter plot for the DAF2DA dye-positive population of RAW264.7 cells, upon transient knockdown of *Odc1* followed by infection with STM WT, the data is determined by flow-cytometry post-staining the infected macrophages with the dye, D. The quantification of (C), E. The fold proliferation of STM WT upon infection into primary macrophages isolated from *iNOS-/-* mice followed by treatment with DFMO (data is from one experiment representative of 3 independent experiments), F. The experimental procedure to study the organ burden of STM WT in C57BL/6 mice upon treatment with DFMO, G-J. The organ burden of STM WT in the Intestine, MLN, Spleen and Liver of C57BL/6 mice upon intraperitoneal treatment of DFMO (2mg/mice and 1mg/mice) as mentioned in (E), K. Experimental procedure used to study the survival of C57BL/6 mice upon infection with STM WT and treatment with DFMO, L. The survival of C57BL/6 mice upon infection with STM and intraperitoneal treatment of DFMO (2mg/mice and 1mg/mice) as mentioned in (J), M. Hematoxylin and eosin staining of histopathological sections of liver upon DFMO treatment to C57BL/6 mice (N=5, scale bar-50μM). Here, (IC) Multiple aggregations of inflammatory cells dispersed in the liver parenchyma, (N) shows several small necrotic areas, (C) congestion and damage to the endothelial lining of the central vein, (HPV) congestion of the hepatic portal vein. The disease score index for liver tissue damage upon STM WT infection in C57BL/6 mice with DFMO treatment. The disease score is as

:0 for normal pathology, 1 for mild/ minor pathology, 2 for moderate pathology, and 3 for severe pathological changes. One-way ANOVA with Dunnet's post-hoc test was used to analyse the data, non-parametric One-way ANOVA (Kruskal Wallis) with Dunn's post-hoc test was used to analyses organ burden; p values ****<0.0001, ***<0.001, **<0.01, *<0.05. Two-way ANOVA with Tukey's post-hoc test was used to analyze the grouped data; p values ****<0.0001, ***<0.001, **<0.01, *<0.05. All data are represented as mean±SD from three independent experiments (N≥3). The survival curve has been analysed using Mantel-Cox log rank method.

Statistical Analysis

Statistical analyses were performed with GraphPad Prism software. All data was tested for normal distribution using Shapiro-Wilk test. The Student's t-test (parametric, two-tailed, unpaired) and One-way ANOVA with Dunnet's post-hoc test were performed as indicated. Two-way ANOVA with Tukey's post-hoc test was used for grouped data. For animal experiments, a Non-parametric One-way ANOVA (Kruskal Wallis) test with Dunn's post-hoc test was performed. The results are expressed as mean ± SD from three independent experiments (N≥ 3). Group sizes and p values for each experiment are described in figure legends.

Discussion

Salmonella is often referred to as a smart pathogen. Over the years, it has developed multiple strategies to combat host-derived stresses (60, 61). A significant part of *Salmonella's* life cycle during its pathogenesis involves residing in the macrophages. This Gram-negative bacteria

experience multiple host-induced environmental stress conditions inside the macrophages (62). Rapid oxidative burst and ROS production are critical mechanisms by which the host macrophages try to limit the invading pathogen. ROS includes superoxide radicals, hydroxyl radicals, peroxy-nitrites, peroxy-chlorides, and hydrogen peroxide. ROS can pass through the bacterial cell wall and act on lipids, proteins, and nucleic acids by oxidizing them and leading to cellular damage. To combat the oxidative burst generated by NOX2 in macrophages, *Salmonella* carries multiple antioxidant enzymes such as the catalases KatE and KatG, the superoxide dismutases SodA and SodB, the Alkyl hydroperoxide reductase, the glutaredoxins and thioredoxins and Hrg transcriptional regulator (35). Polyamines assist in *Salmonella* virulence and aid in stress resistance. However, the mechanism behind the role of polyamines in *Salmonella* stress resistance and virulence remains less appreciated.

Our study identifies spermidine as a stress-responsive regulatory molecule in *Salmonella* Typhimurium. We show spermidine is critical for the survival and proliferation of STM in macrophages and in the presence of oxidative stress *in vitro.* The spermidine transporter and biosynthesis mutants display significantly reduced capability to be phagocytosed by the macrophages. Findings from our previous study showed that the intracellular level of spermidine is substantially less in both the spermidine transport and biosynthesis mutants, which further explains the attenuated proliferation of both the mutants in macrophages (13). The previous findings also showed that in the absence of the transport genes in *Salmonella* Typhimurium, the synthesis genes are downregulated and vice versa. The lack of spermidine transport and biosynthesis diminishes the mRNA expression of multiple arms of oxidative stress response in *Salmonella*, such as those regulated by RpoS, SoxR/S and EmrR, respectively. Numerous studies show the role of polyamines in regulating the transcription of multiple genes by interacting with

DNA in eukaryotes. They bind to the DNA and change conformation as in C-MYC transcription, and in other cases, enhance DNA-protein binding affinities like for Estrogen-response elements (63, 64). Thus, in *Salmonella* Typhimurium, *rpoS*, *soxR,* and *emrR* similarly fall under the "Polyamine modulon".

We further characterise a novel enzyme, GspSA, in *Salmonella* Typhimurium, which synthesises a conjugated product of glutathione (GSH) and spermidine called GS-sp. GspSA is critical for *Salmonella* Typhimurium to survive and proliferate in macrophages. Our study shows that the absence of GspSA attenuates the survival of STM under oxidative stress conditions *in vitro,* suggesting a vital role of GspSA in protecting STM from oxidative damage. GS-sp in *E. coli* carries out its function by modifying protein thiol groups under oxidative stress to protect the proteins from getting oxidised and damaged. In *Salmonella* Typhimurium, we further show that the spermidine regulates the *gsp* expression and the subsequent production of GS-sp. We expect that GS-sp generated under oxidative stress conditions and inside the macrophages likewise interact with cysteine-thiol groups in proteins to shield them from oxidative damage. MK Chattopadhyay (2013) showed that this enzyme (GspSA) is specifically present in two groups of organisms, namely bacteria and kinetoplastids, respectively, and completely absent in other organisms such as humans, rats, drosophila, etc., among the bacteria group in all *enterobacteria* showed 27-100% homology and >65% identity in around 50% of the species, with *E. coli* (40). Thus, the absence of GspSA in eukaryotes makes it a potent drug target for treating *Salmonella* infections. Thus, spermidine exerts pleiotropic effects in *Salmonella* by manipulates the multiple arms of antioxidative response. Our study gives a mechanistic insight into spermidine's regulation under oxidative stress. Spermidine regulates *rpoS, soxR* and *emrR* transcription factors and their downstream antioxidative enzymes. However, the absence of spermidine has a prominent effect

on the expression of superoxide dismutases (*sodA* and *sodB*) and glutathione synthase enzymes. It strengthens the bacteria to cope with hostile host environments, such as the high ROS levels generated by the NOX2 enzyme in macrophages. Our studies in the *in vivo* model of *Salmonella* Typhimurium infection further dissect the role of spermidine in assisting in the pathogenesis by potentiating its ability to cope with the oxidative stress and thus enhancing its virulence strategies. The observation of higher fold proliferation of the spermidine mutants in peritoneal macrophages isolated from NOX2 knockout mice (*gp91phox-/-* mice) also corroborates with the role of spermidine in oxidative stress response. Considering our multiple mutants, we find that the spermidine transporter mutant does not show statistically significant reduced colonization compared to the other mutants in the liver upon oral gavage. However, the trend shows lesser colonization by this mutant. On the other hand, the *gsp* mutant also does not have a statistically significant difference in its ability to disseminate in blood, while the trend shows less dissemination than STM WT. Thus, a subtle difference is observed among the mutants through our *in vivo* study, suggesting the minute variance among the mutants themselves. Moreover, it is at the nexus of multiple oxidative stress response arms in *Salmonella*, thereby assisting in mounting an antioxidative response to promote its survival in macrophages.

Studies in the past have offered insights into the function of polyamines in the pathogenesis of multiple virulent bacteria. Many human pathogenic bacteria have developed ways to exploit, interfere and manipulate the polyamine metabolism of the host to enhance their fitness within the niche. As in *Shigella* and *Vibrio spp.* polyamines produced by the bacteria are critical in determining virulence (65, 66). Meanwhile, bacteria such as *Legionella spp*., which does not synthesize polyamines, depend on the host-acquired polyamines for their pathogenesis (67). Another unique mechanism is observed in *H. pylori,* which activates polyamine oxidation, thereby

dysregulating the innate immune response (68). Also, in response to *H. pylori* infection, the host macrophages increase the arginase activity and ornithine decarboxylase activity to produce polyamines (69). A recent study showed that SARS-Cov-2 hijacks the host polyamines for reproduction and infection (70).

Our findings also reveal that *Salmonella* Typhimurium enhances the polyamine production in the host upon infection using its specialized pathogenicity island encoded effectors from SPI-1 and SPI-2, which might be a strategy to hijack the host polyamines for its survival. This further explains another reason for the reduced proliferation observed for the spermidine transport mutant in macrophages. Also, the knockdown of host ornithine decarboxylase attenuates *Salmonella* proliferation in macrophages. The upregulation of Odc1 activity manages to feed the amino acid, L-arginine, into the polyamine biosynthesis and prevent nitric oxide production, which otherwise would be detrimental for the pathogen. Polyamines have been well-studied as a drug target for the treatment of multiple cancers. The oncogene MYC is upregulated in 70 per cent of the cancer types. Ornithine decarboxylase (Odc1), a rate-limiting enzyme of polyamine biosynthesis, is transcriptionally activated directly by MYC, thereby increasing Odc1 levels in cancer (71). RAS is another essential factor in cell growth and cancer development, and it acts on Odc1 to activate Odc1 in cancer cells translationally (72). Polyamine biosynthesis is also associated with other pathways, such as AKT and mTORC pathways (73, 74). Previous studies show that D, L-α-difluoromethylornithine (DFMO) can be useful in treating various cancers (54). It acts as a suicide inhibitor of the rate-limiting enzyme Odc1 in the polyamine biosynthesis pathway (58). Studies suggest that it restricts the use of arginine for polyamine biosynthesis. Arginine is the common precursor to polyamine biosynthesis and nitric oxide synthesis. Thus, blocking polyamine biosynthesis enhances nitric oxide ($NO^{\cdot}$) production (75). Nitric oxide is generated from the

inducible Nitric oxide synthase (NOS2) enzyme in macrophages as an innate immune response to invading pathogens or inflammation (76). The NO˚ radical is a labile molecule that reacts with peroxides and thiols to produce highly reactive species of peroxynitrites and nitrosothiols to control the infection by the invading pathogen, including *Salmonella* (7, 77). It also acts on nucleic acids, leading to deamination and mutagenesis (76). Our study shows that upon using mOdc1 suicide inhibitor, DFMO, *Salmonella* proliferation could be diminished, and it reduces the bacterial burden in mice. The FDA-approved chemo-preventive drug, DFMO, for Human African Trypanosomiasis treatment is a potential drug to cure *Salmonella* infection by blocking host polyamine biosynthesis and moreover enhancing the NO production in macrophages. In the devastating age of increasing antibiotic resistance, such a drug promises to combat deadly pathogens like *Salmonella* effectively.

Though this study underlines the role and mechanism of spermidine's anti-oxidative role in Salmonella, it bears a few limitations. Firstly, our study shows the changes in the expression of various antioxidative genes at the mRNA levels in the spermidine transport and biosynthesis mutants in *Salmonella.* However, it does not reveal precisely how spermidine regulates expression. We speculate in regard to the published literature on spermidine's interaction with nucleic acids and its role in the regulation of transcription and translation, that the observation from our study might also be from a similar mode of regulation by spermidine (78). Future studies on understanding the mechanism of interaction of spermidine with these genes will provide further mechanistic depth to our observation. Secondly, our study confirmed that *Salmonella* employs the effectors encoded by the SPI-1 and SPI-2 to modulate the host polyamine metabolic pathway. However, which effectors are critical in the modulation of the host remains unanswered. In order

to unravel the critical effectors involved in the upregulation of the host polyamine biosynthesis pathway further research is necessary.

Impact of the research in the advancement of knowledge or benefit to mankind

A substantial duration of the infection cycle of *Salmonella* involves the macrophages, which present a very hostile environment to the bacteria. However, *Salmonella* can survive and proliferate within host macrophages and utilize it to disseminate to secondary sites of infection. Our study identifies a novel strategy employed by *Salmonella* Typhimurium to counteract oxidative and nitrosative stress within the host. We demonstrate that spermidine is a critical regulatory molecule in *Salmonella* that regulates multiple antioxidative pathways along with a novel antioxidative enzyme (GspSA) in *Salmonella* to prevent oxidative damage and assist in its virulence in mice. It further rewires host polyamine metabolism in a SPI-1 and SPI-2-dependent manner to prevent nitric oxide production and enhance survival. In the era of antimicrobial resistance, this study further recognizes an FDA-approved chemo-preventive drug, DFMO, which inhibits the host-polyamine metabolism, as a prospective antidote to treat *Salmonella* infection.

The fluoroquinolone-resistant *Salmonella* Typhi and Non-typhoidal serovars have been listed as the “High priority” pathogen by WHO in 2024. Further, the rise of antibiotic resistance is increasing at an alarming rate across the world. A study published in The Lancet, 2022 highlighted the emergence of these multi-drug resistant (MDR) and extensively-drug resistant (XDR) *Salmonella* Typhi in Pakistan. Also, it showed that these lineages originated in the Indian subcontinent, and since 1990, it has spread to other countries almost 200 times. The pathogen is genetically evolving by gaining resistance genes to various classes of antibiotics such as

ampicillin, chloramphenicol, trimethoprim and sulfamethoxazole. Recently, XDR strains with resistance to fluoroquinolones and third-generation cephalosporins have also been reported. Our current research shows the potential of the FDA-approved drug DFMO, in preventing *Salmonella* infection in the host. This serves as an "Alternative Therapeutic strategy", where we are not directly targeting the bacteria but inhibiting the host metabolic pathway. This does not allow the bacteria to mutate and evolve resistance to the drug genetically. Thus, in the devastating age of antimicrobial resistance, DFMO serves as a curative drug against *Salmonella* infection.

Literature references

1. Hernandez DJ, David AS, Menges ES, Searcy CA, Afkhami ME. Environmental stress destabilizes microbial networks. The ISME Journal. 2021;15(6):1722-34.
2. Gray DA, Dugar G, Gamba P, Strahl H, Jonker MJ, Hamoen LW. Extreme slow growth as alternative strategy to survive deep starvation in bacteria. Nature communications. 2019;10(1):890.
3. Winfield MD, Groisman EA. Role of nonhost environments in the lifestyles of Salmonella and Escherichia coli. Applied and environmental microbiology. 2003;69(7):3687-94.
4. Dodd CE, Richards PJ, Aldsworth TG. Suicide through stress: a bacterial response to sub-lethal injury in the food environment. International journal of food microbiology. 2007;120(1-2):46-50.
5. Marmion M, Macori G, Ferone M, Whyte P, Scannell A. Survive and thrive: Control mechanisms that facilitate bacterial adaptation to survive manufacturing-related stress. International Journal of Food Microbiology. 2022;368:109612.
6. Vazquez-Torres A, Fang FC. Salmonella evasion of the NADPH phagocyte oxidase. Microbes and infection. 2001;3(14-15):1313-20.
7. Chakravortty D, Hansen-Wester I, Hensel M. Salmonella pathogenicity island 2 mediates protection of intracellular Salmonella from reactive nitrogen intermediates. The Journal of experimental medicine. 2002;195(9):1155-66.
8. Rhee H, Kim EJ, Lee J. Physiological polyamines: simple primordial stress molecules. Journal of cellular and molecular medicine. 2007;11(4):685-703.
9. Barbagallo M, Di Martino ML, Marcocci L, Pietrangeli P, De Carolis E, Casalino M, et al. A new piece of the Shigella pathogenicity puzzle: spermidine accumulationby silencing of the speG gene. PloS one. 2011;6(11):e27226.
10. Johnson L, Mulcahy H, Kanevets U, Shi Y, Lewenza S. Surface-localized spermidine protects the Pseudomonas aeruginosa outer membrane from antibiotic treatment and oxidative stress. Journal of bacteriology. 2012;194(4):813-26.

11. Banerji R, Iyer P, Saroj SD. Spermidine enhances the survival of Streptococcus pyogenes M3 under oxidative stress. Molecular Oral Microbiology. 2022;37(2):53-62.
12. Espinel IC, Guerra PR, Jelsbak L. Multiple roles of putrescine and spermidine in stress resistance and virulence of Salmonella enterica serovar Typhimurium. Microbial pathogenesis. 2016;95:117-23.
13. Nair AV, Devasurmutt Y, Rahman SA, Tatu US, Chakravortty D. Spermidine facilitates the adhesion and subsequent invasion of Salmonella Typhimurium into epithelial cells via the regulation of surface adhesive structures and the SPI-1. bioRxiv. 2023:2023.06. 03.543567.
14. Nair AV, Singh A, Devasurmutt Y, Rahman S, Tatu US, Chakravortty D. Spermidine constitutes a key determinant of motility and attachment of Salmonella Typhimurium through a novel regulatory mechanism. Microbiological Research. 2024:127605.
15. Datsenko KA, Wanner BL. One-step inactivation of chromosomal genes in Escherichia coli K-12 using PCR products. Proceedings of the National Academy of Sciences. 2000;97(12):6640-5.
16. Roy Chowdhury A, Sah S, Varshney U, Chakravortty D. Salmonella Typhimurium outer membrane protein A (OmpA) renders protection from nitrosative stress of macrophages by maintaining the stability of bacterial outer membrane. PLoS pathogens. 2022;18(8):e1010708.
17. Chandra K, Roy Chowdhury A, Chatterjee R, Chakravortty D. GH18 family glycoside hydrolase Chitinase A of Salmonella enhances virulence by facilitating invasion and modulating host immune responses. PLoS pathogens. 2022;18(4):e1010407.
18. Chatterjee R, Chaudhuri D, Setty SRG, Chakravortty D. Deceiving The Big Eaters: Salmonella Typhimurium SopB subverts host cell Xenophagy in macrophages via dual mechanisms. Microbes and infection. 2023:105128.
19. Liu T-H, Yaghmour MA, Lee M-H, Gradziel TM, Leveau JH, Bostock RM. An roGFP2-based bacterial bioreporter for redox sensing of plant surfaces. Phytopathology. 2020;110(2):297-308.
20. Bhaskar A, Munshi M, Khan SZ, Fatima S, Arya R, Jameel S, et al. Measuring glutathione redox potential of HIV-1-infected macrophages. Journal of Biological Chemistry. 2015;290(2):1020-38.
21. Chatterjee R, Nair AV, Singh A, Mehta N, Setty SRG, Chakravortty D. Syntaxin 3 SPI-2 dependent crosstalk facilitates the division of Salmonella containing vacuole. Traffic. 2023.
22. Roy Chowdhury A, Sah S, Varshney U, Chakravortty D. Salmonella Typhimurium outer membrane protein A (OmpA) renders protection from nitrosative stress of macrophages by maintaining the stability of bacterial outer membrane. PLoS Pathogens. 2022;18(8):e1010708.
23. Salbitani G, Bottone C, Carfagna S. Determination of reduced and total glutathione content in extremophilic microalga Galdieria phlegrea. Bio-protocol. 2017;7(13):e2372-e.
24. Saydjari R, Alexander RW, Upp JR, Poston GJ, Barranco SC, Townsend CM, et al. The effect of tumor burden on ornithine decarboxylase activity in mice. Cancer investigation. 1991;9(4):415-9.
25. Aziz F, Xin M, Gao Y, Chakroborty A, Khan I, Monts J, et al. Induction and prevention of gastric cancer with combined Helicobacter pylori and capsaicin administration and DFMO treatment, respectively. Cancers. 2020;12(4):816.
26. Mitchison D, Wallace J, Bhatia A, Selkon J, Subbaiah T, Lancaster M. A comparison of the virulence in guinea-pigs of South Indian and British tubercle bacilli. Tubercle. 1960;41(1):1-22.

27. Achouri S, Wright JA, Evans L, Macleod C, Fraser G, Cicuta P, et al. The frequency and duration of Salmonella–macrophage adhesion events determines infection efficiency. Philosophical Transactions of the Royal Society B: Biological Sciences. 2015;370(1661):20140033.
28. Kim J-S, Liu L, Davenport B, Kant S, Morrison TE, Vazquez-Torres A. Oxidative stress activates transcription of Salmonella pathogenicity island-2 genes in macrophages. Journal of Biological Chemistry. 2022;298(7).
29. Miller JF, Mekalanos JJ, Falkow S. Coordinate regulation and sensory transduction in the control of bacterial virulence. Science. 1989;243(4893):916-22.
30. Chattopadhyay MK, Keembiyehetty CN, Chen W, Tabor H. Polyamines stimulate the level of the σ38 subunit (RpoS) of Escherichia coli RNA polymerase, resulting in the induction of the glutamate decarboxylase-dependent acid response system via the gadE regulon. Journal of Biological Chemistry. 2015;290(29):17809-21.
31. Kashiwagi K, Yamaguchi Y, Sakai Y, Kobayashi H, Igarashi K. Identification of the polyamine-induced protein as a periplasmic oligopeptide binding protein. Journal of Biological Chemistry. 1990;265(15):8387-91.
32. Sakamoto A, Terui Y, Yoshida T, Yamamoto T, Suzuki H, Yamamoto K, et al. Three members of polyamine modulon under oxidative stress conditions: two transcription factors (SoxR and EmrR) and a glutathione synthetic enzyme (GshA). PLoS One. 2015;10(4):e0124883.
33. Farr SB, Kogoma T. Oxidative stress responses in Escherichia coli and Salmonella typhimurium. Microbiological reviews. 1991;55(4):561-85.
34. Storz G, Tartaglia LA, Farr SB, Ames BN. Bacterial defenses against oxidative stress. Trends in Genetics. 1990;6:363-8.
35. Rhen M. Salmonella and reactive oxygen species: a love-hate relationship. Journal of innate immunity. 2019;11(3):216-26.
36. Song M, Husain M, Jones-Carson J, Liu L, Henard CA, Vázquez-Torres A. Low-molecular-weight thiol-dependent antioxidant and antinitrosative defences in S almonella pathogenesis. Molecular microbiology. 2013;87(3):609-22.
37. Bollinger JM, Kwon DS, Huisman GW, Kolter R, Walsh CT. Glutathionylspermidine Metabolism in Escherichia coli.: PURIFICATION, CLONING, OVERPRODUCTION, AND CHARACTERIZATION OF A BIFUNCTIONAL GLUTATHIONYLSPERMIDINE SYNTHETASE/AMIDASE∗. Journal of Biological Chemistry. 1995;270(23):14031-41.
38. Krauth-Siegel RL, Lüdemann H. Reduction of dehydroascorbate by trypanothione. Molecular and biochemical parasitology. 1996;80(2):203-8.
39. Ariyanayagam MR, Fairlamb AH. Ovothiol and trypanothione as antioxidants in trypanosomatids. Molecular and biochemical parasitology. 2001;115(2):189-98.
40. Chattopadhyay MK, Chen W, Tabor H. Escherichia coli glutathionylspermidine synthetase/amidase: phylogeny and effect on regulation of gene expression. FEMS microbiology letters. 2013;338(2):132-40.
41. Wyllie S, Oza SL, Patterson S, Spinks D, Thompson S, Fairlamb AH. Dissecting the essentiality of the bifunctional trypanothione synthetase-amidase in Trypanosoma brucei using chemical and genetic methods. Molecular microbiology. 2009;74(3):529-40.

42. Kerrinnes T, Winter MG, Young BM, Diaz-Ochoa VE, Winter SE, Tsolis RM. Utilization of host polyamines in alternatively activated macrophages promotes chronic infection by Brucella abortus. Infection and immunity. 2018;86(3):10.1128/iai. 00458-17.
43. Forest CG, Ferraro E, Sabbagh SC, Daigle F. Intracellular survival of Salmonella enterica serovar Typhi in human macrophages is independent of Salmonella pathogenicity island (SPI)-2. Microbiology. 2010;156(12):3689-98.
44. Ellermeier JR, Slauch JM. Adaptation to the host environment: regulation of the SPI1 type III secretion system in Salmonella enterica serovar Typhimurium. Current opinion in microbiology. 2007;10(1):24-9.
45. Brawn LC, Hayward RD, Koronakis V. Salmonella SPI1 effector SipA persists after entry and cooperates with a SPI2 effector to regulate phagosome maturation and intracellular replication. Cell host & microbe. 2007;1(1):63-75.
46. Giacomodonato MN, Uzzau S, Bacciu D, Caccuri R, Sarnacki SH, Rubino S, et al. SipA, SopA, SopB, SopD and SopE2 effector proteins of Salmonella enterica serovar Typhimurium are synthesized at late stages of infection in mice. Microbiology. 2007;153(4):1221-8.
47. Brown NF, Vallance BA, Coombes BK, Valdez Y, Coburn BA, Finlay BB. Salmonella pathogenicity island 2 is expressed prior to penetrating the intestine. PLoS pathogens. 2005;1(3):e32.
48. Kingsnorth A, Lumsden AB, Wallace HM. Polyamines in colorectal cancer. Journal of British Surgery. 1984;71(10):791-4.
49. Evageliou NF, Hogarty MD. Disrupting polyamine homeostasis as a therapeutic strategy for neuroblastoma. Clinical Cancer Research. 2009;15(19):5956-61.
50. Tsoi T-H, Chan C-F, Chan W-L, Chiu K-F, Wong W-T, Ng C-F, et al. Urinary polyamines: a pilot study on their roles as prostate cancer detection biomarkers. PLoS One. 2016;11(9):e0162217.
51. Choi Y, Oh ST, Won M-A, Choi KM, Ko MJ, Seo D, et al. Targeting ODC1 inhibits tumor growth through reduction of lipid metabolism in human hepatocellular carcinoma. Biochemical and biophysical research communications. 2016;478(4):1674-81.
52. Soda K. The mechanisms by which polyamines accelerate tumor spread. Journal of Experimental & Clinical Cancer Research. 2011;30:1-9.
53. Weeks C, Herrmann A, Nelson F, Slaga T. alpha-Difluoromethylornithine, an irreversible inhibitor of ornithine decarboxylase, inhibits tumor promoter-induced polyamine accumulation and carcinogenesis in mouse skin. Proceedings of the National Academy of Sciences. 1982;79(19):6028-32.
54. Horn Y, Schechter PJ, Marton LJ. Phase I–II clinical trial with alpha-difluoromethylornithine—an inhibitor of polyamine biosynthesis. European Journal of Cancer and Clinical Oncology. 1987;23(8):1103-7.
55. Lewis EC, Kraveka JM, Ferguson W, Eslin D, Brown VI, Bergendahl G, et al. A subset analysis of a phase II trial evaluating the use of DFMO as maintenance therapy for high-risk neuroblastoma. International journal of cancer. 2020;147(11):3152-9.
56. Roberts S, Ullman B. Parasite polyamines as pharmaceutical targets. Current Pharmaceutical Design. 2017;23(23):3325-41.

57. Eperon G, Balasegaram M, Potet J, Mowbray C, Valverde O, Chappuis F. Treatment options for second-stage gambiense human African trypanosomiasis. Expert review of anti-infective therapy. 2014;12(11):1407-17.
58. Li H, Meininger CJ, Kelly KA, Hawker Jr JR, Morris Jr SM, Wu G. Activities of arginase I and II are limiting for endothelial cell proliferation. American Journal of Physiology-Regulatory, Integrative and Comparative Physiology. 2002;282(1):R64-R9.
59. Bojarska J, New R, Borowiecki P, Remko M, Breza M, Madura ID, et al. The first insight into the supramolecular system of D, L-α-difluoromethylornithine: A new antiviral perspective. Frontiers in Chemistry. 2021;9:679776.
60. Buchmeier NA, Heffron F. Induction of Salmonella stress proteins upon infection of macrophages. Science. 1990;248(4956):730-2.
61. Shen S, Fang FC. Integrated stress responses in Salmonella. International journal of food microbiology. 2012;152(3):75-81.
62. HaragaA OM. MillerSI. Salmonellaeinterplaywith hostcells. 2008;6(1):53G66.
63. Kumar N, Basundra R, Maiti S. Elevated polyamines induce c-MYC overexpression by perturbing quadruplex–WC duplex equilibrium. Nucleic acids research. 2009;37(10):3321-31.
64. Thomas T, Gallo MA, Klinge CM, Thomas T. Polyamine-mediated conformational perturbations in DNA alter the binding of estrogen receptor to poly (dG-m5dC). poly (dG-m5dC) and a plasmid containing the estrogen response element. The Journal of Steroid Biochemistry and Molecular Biology. 1995;54(3-4):89-99.
65. Prosseda G, Di Martino ML, Campilongo R, Fioravanti R, Micheli G, Casalino M, et al. Shedding of genes that interfere with the pathogenic lifestyle: the Shigella model. Research in microbiology. 2012;163(6-7):399-406.
66. Lee J, Sperandio V, Frantz DE, Longgood J, Camilli A, Phillips MA, et al. An alternative polyamine biosynthetic pathway is widespread in bacteria and essential for biofilm formation in Vibrio cholerae. Journal of Biological Chemistry. 2009;284(15):9899-907.
67. Nasrallah GK, Riveroll AL, Chong A, Murray LE, Lewis PJ, Garduno RA. Legionella pneumophila requires polyamines for optimal intracellular growth. Journal of bacteriology. 2011;193(17):4346-60.
68. Chaturvedi R, Asim M, Romero–Gallo J, Barry DP, Hoge S, De Sablet T, et al. Spermine oxidase mediates the gastric cancer risk associated with Helicobacter pylori CagA. Gastroenterology. 2011;141(5):1696-708. e2.
69. Chaturvedi R, Cheng Y, Asim M, Bussière FI, Xu H, Gobert AP, et al. Induction of polyamine oxidase 1 by Helicobacter pylori causes macrophage apoptosis by hydrogen peroxide release and mitochondrial membrane depolarization. Journal of Biological Chemistry. 2004;279(38):40161-73.
70. Makhoba XH, Makumire S. The capture of host cell's resources: The role of heat shock proteins and polyamines in SARS-COV-2 (COVID-19) pathway to viral infection. Biomolecular Concepts. 2022;13(1):220-9.
71. Bachmann AS, Geerts D. Polyamine synthesis as a target of MYC oncogenes. Journal of Biological Chemistry. 2018;293(48):18757-69.
72. Origanti S, Shantz LM. Ras transformation of RIE-1 cells activates cap-independent translation of ornithine decarboxylase: regulation by the Raf/MEK/ERK and phosphatidylinositol 3-kinase pathways. Cancer research. 2007;67(10):4834-42.

73. Gomes AP, Schild T, Blenis J. Adding polyamine metabolism to the mTORC1 toolkit in cell growth and cancer. Developmental cell. 2017;42(2):112-4.
74. Dai F, Yu W, Song J, Li Q, Wang C, Xie S. Extracellular polyamines-induced proliferation and migration of cancer cells by ODC, SSAT, and Akt1-mediated pathway. Anti-Cancer Drugs. 2017;28(4):457-64.
75. Bauer PM, Buga GM, Fukuto JM, Pegg AE, Ignarro LJ. Nitric Oxide Inhibits Ornithine Decarboxylase viaS-Nitrosylation of Cysteine 360 in the Active Site of the Enzyme. Journal of Biological Chemistry. 2001;276(37):34458-64.
76. Bogdan C. Nitric oxide synthase in innate and adaptive immunity: an update. Trends in immunology. 2015;36(3):161-78.
77. Okamoto T, Gohil K, Finkelstein EI, Bove P, Akaike T, Van Der Vliet A. Multiple contributing roles for NOS2 in LPS-induced acute airway inflammation in mice. American Journal of Physiology-Lung Cellular and Molecular Physiology. 2004;286(1):L198-L209.
78. Yoshida M, Meksuriyen D, Kashiwagi K, Kawai G, Igarashi K. Polyamine stimulation of the synthesis of oligopeptide-binding protein (OppA): Involvement of a structural change of the Shine-Dalgarno sequence and the initiation codon aug in oppa mRNA. Journal of Biological Chemistry. 1999;274(32):22723-8.

Figure S1: Spermidine aids in the proliferation and survival of *Salmonella* Typhimurium in macrophages

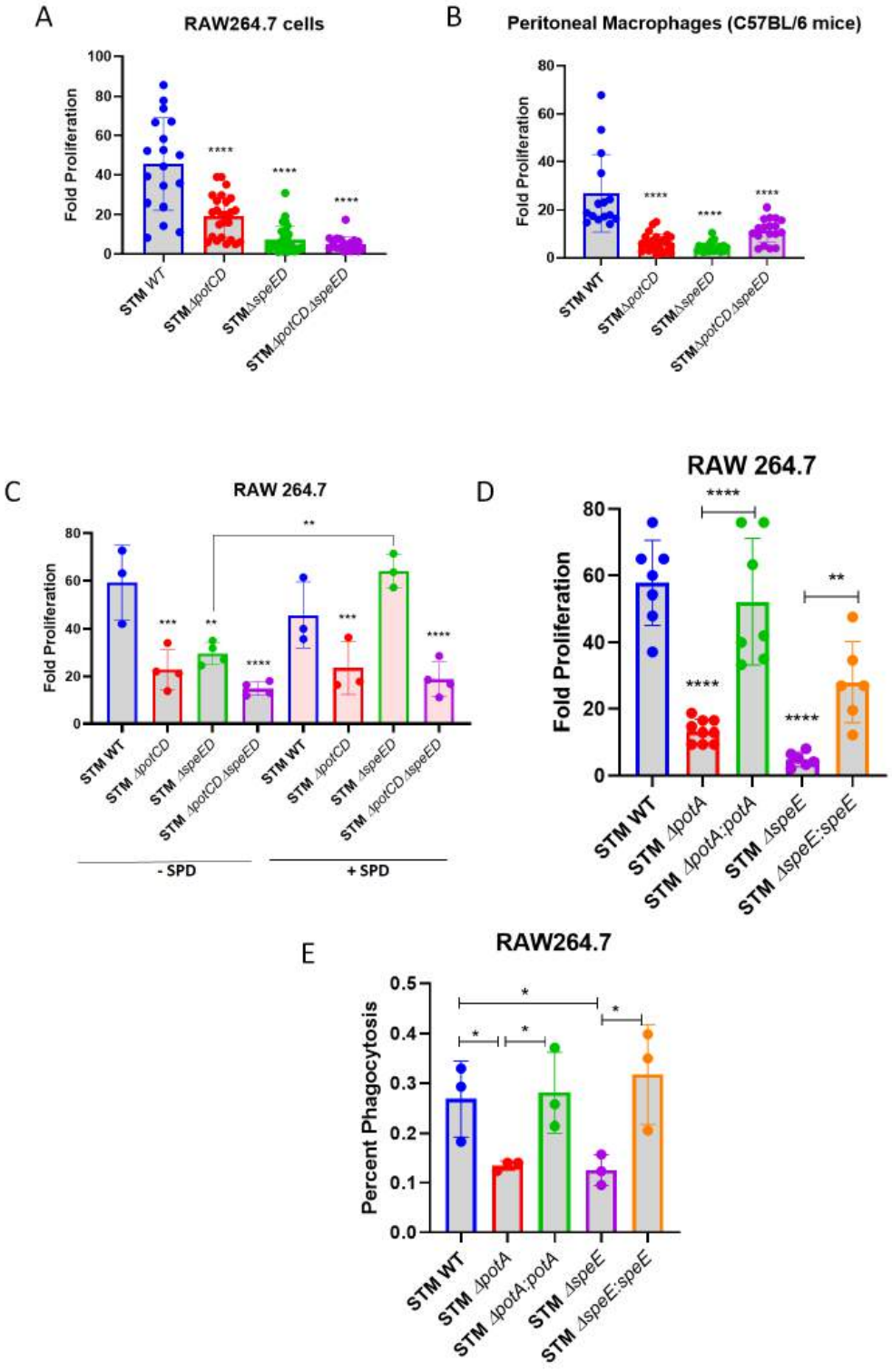

Figure S1 Spermidine aids in the proliferation and survival of *Salmonella* Typhimurium in macrophages:

A. The fold proliferation of spermidine mutants in RAW264.7 cells (data is from one experiment representative of 3 independent experiments), B. The fold proliferation in primary macrophages isolated from the peritoneal lavage of C57BL/6 (data is from one experiment representative of 3 independent experiments), C. The fold proliferation of the spermidine mutants grown in media supplemented with 100μM spermidine (SPD) prior to infection, D. The fold proliferation of spermidine mutant complemented strains in RAW264.7 cells (data is from one experiment representative of 3 independent experiments), E. The percentage phagocytosis of spermidine mutant complemented strains in RAW264.7 cells. One-way ANOVA with Dunnet's post-hoc test was used to analyze the data; p values****<0.0001, ***<0.001, **<0.01. All data are represented as mean±SD from three independent experiments (N≥3).

Figure S2: The antioxidative role of spermidine in *Salmonella* Typhimurium

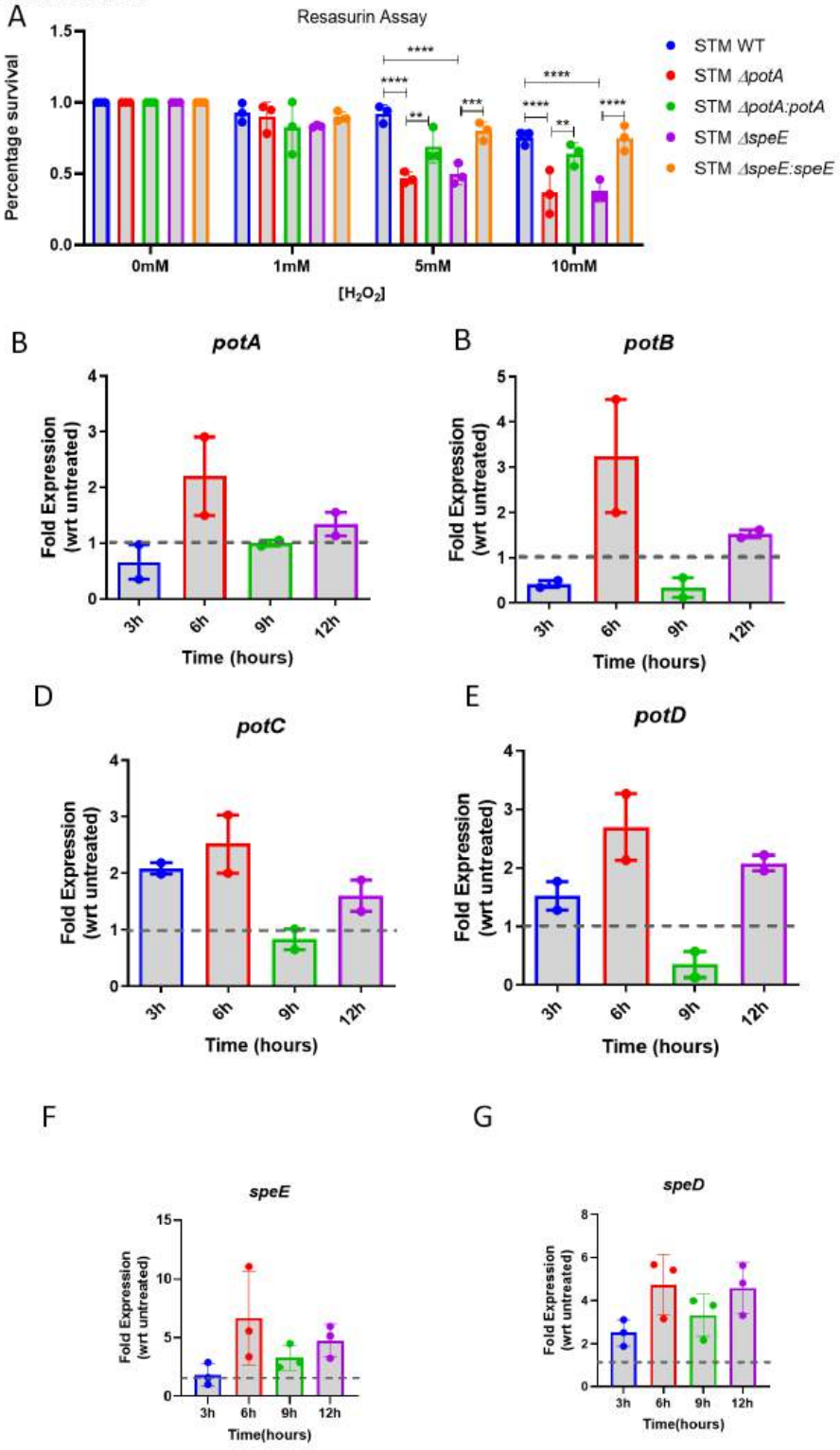

Figure S2: The antioxidative role of spermidine in *Salmonella* Typhimurium

A. The hydrogen peroxide sensitivity assay of spermidine mutant complemented strains *in vitro* by Resazurin assay, B.The mRNA expression of *potA,* C. *potB,* D. *potC,* E. *potD* in STM WT during its *in vitro* growth in LB media with exposure to oxidative stress (1mM Hydrogen peroxide), Data is normalized to internal control of 16S and represented with respect to the untreated (no hydrogen peroxide), F.The mRNA expression of *speE,* G. *speD* in STM WT during its *in vitro* growth in LB media with exposure to oxidative stress (1mM Hydrogen peroxide), Data is normalized to internal control of 16S and represented with respect to the untreated (no hydrogen peroxide). One-way ANOVA with Dunnet's post-hoc test was used to analyze the data; p values ****<0.0001, ***<0.001, **<0.01. All data are represented as mean±SD from three independent experiments (N≥3).

Figure S3: Spermidine regulates the various antioxidative arms in *Salmonella* Typhimurium

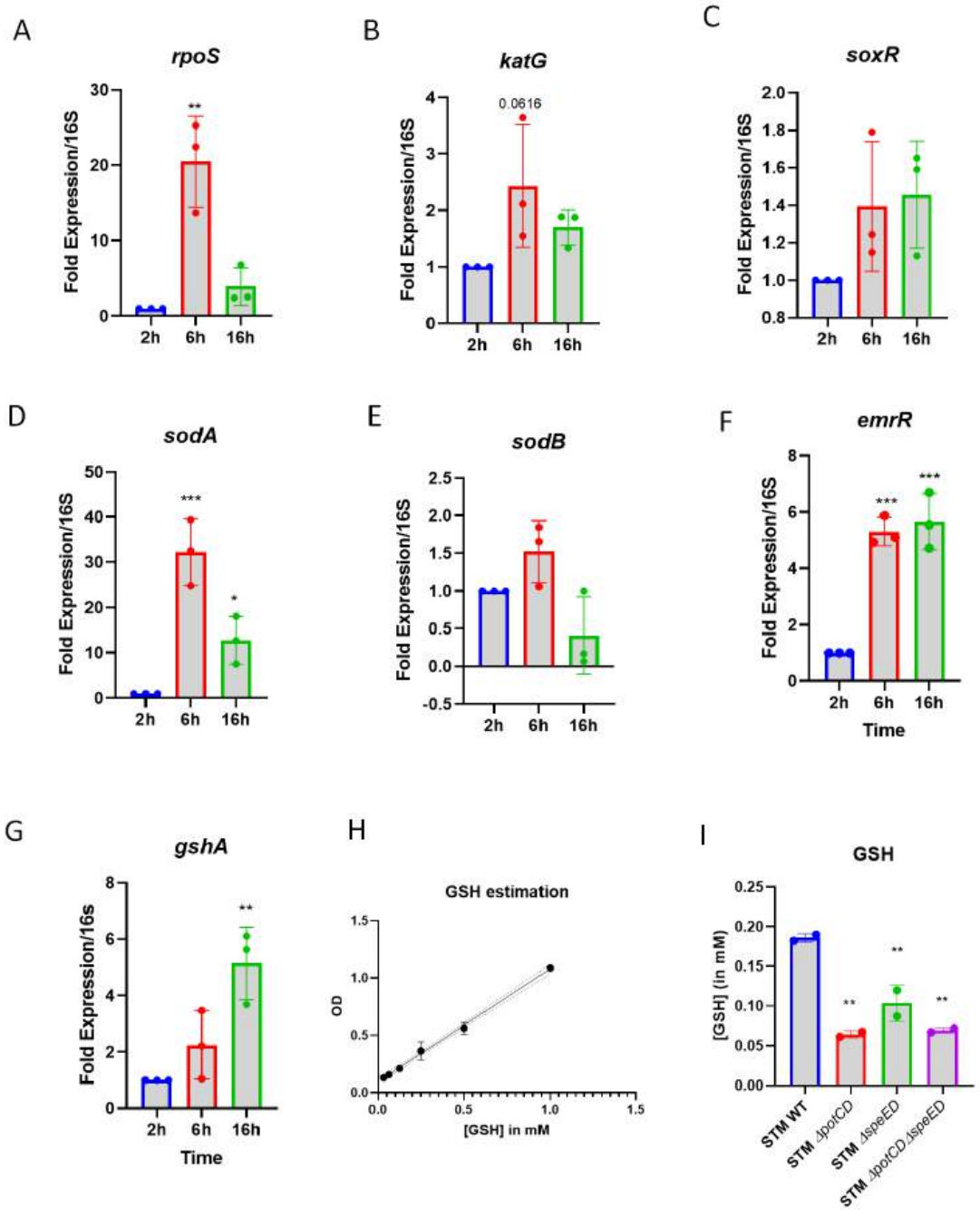

Figure S3: Spermidine regulates the various antioxidative arms in *Salmonella* Typhimurium

The mRNA expression in STM WT upon infection into RAW264.7 cells for various antioxidative genes and their transcription factors A. *rpoS*, B. *katG,* C. *soxR,* D. *sodA,* E. *sodB,* F. *emrR,* G. *gshA.* H. Standard curve for Glutathione (GSH) estimation, I. The intracellular GSH concentration determination in spermidine mutants. One-way ANOVA with Dunnet's post-hoc test was used to analyze the data; p values ****<0.0001, ***<0.001, **<0.01 All data are represented as mean±SD from three independent experiments (N≥3).

Figure S4: GspSA is a novel antioxidative enzyme in *Salmonella* Typhimurium

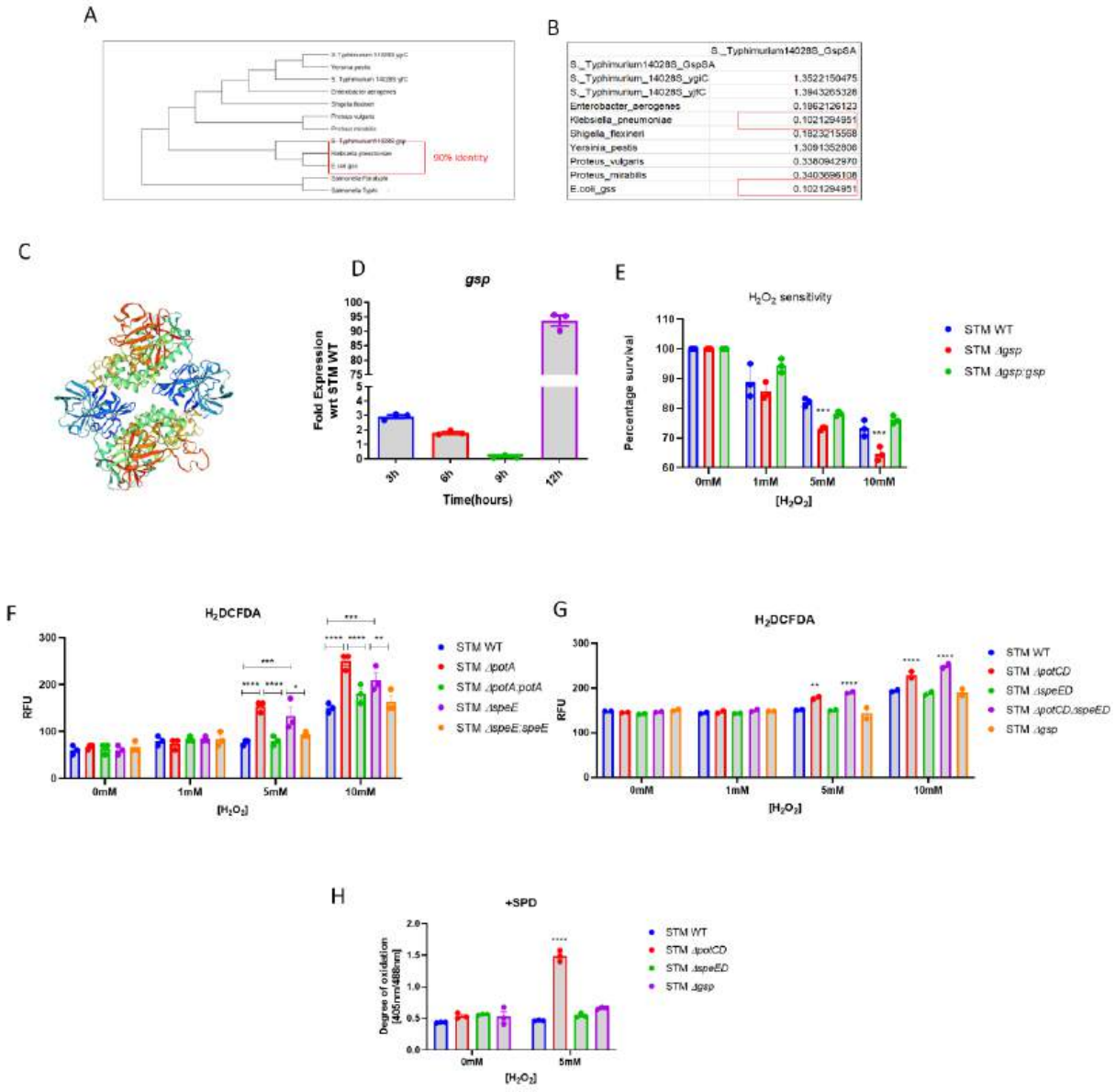

Figure S4: GspSA is a novel antioxidative enzyme in *SalmonellaTyphimurium*

A. The maximum likelihood tree for GspSA of *Salmonella* Typhimurium 14028S with other members of *Enterobacteriaceae* family, B. The pairwise distance of GspSA in *Salmonella* Typhimurium 14028S from other members of *Enterobacteriaceae* family, C. The prediction of

structure using SWISS MODEL , the structure of GspSA in *Salmonella* Typhimurium depicts a homo-dimer with GMQE of 0.93 and QMEANisCo Global of 0.88± 0.05, D. The mRNA expression of *gsp* in STM WT during its *in vitro* growth in LB media upon exposure of 1mM hydrogen peroxide, E. The *in vitro* sensitivity assay of STM WT, STM Δ*gsp* and STM Δ*gsp*:*gsp* in a gradient concentration of hydrogen peroxide (the representative image of one time experiment of N=3, plotted as ±SD), F. The intracellular reactive oxygen species determination using H2DCFDA of spermidine mutant complemented (data is from one experiment representative of 3 independent experiments), G. The intracellular reactive oxygen species determination using H2DCFDA of all the strains grown with supplementation of 100µM spermidine (SPD) (data is from one experiment representative of 3 independent experiments), H. The intracellular redox status determination using ro-GFP2 in all the strains grown with supplementation of 100µM spermidine (SPD). One-way ANOVA with Dunnet's post-hoc test was used to analyze the data; p values****<0.0001, ***<0.001, **<0.01, *<0.05. Two-way ANOVA with Tukey's post-hoc test was used to analyze the grouped data; p values ****<0.0001, ***<0.001, **<0.01, *<0.05. All data are represented as mean±SD from three independent experiments (N≥3).

Figure S5: Spermidine regulates GspSA in *Salmonella* Typhimurium

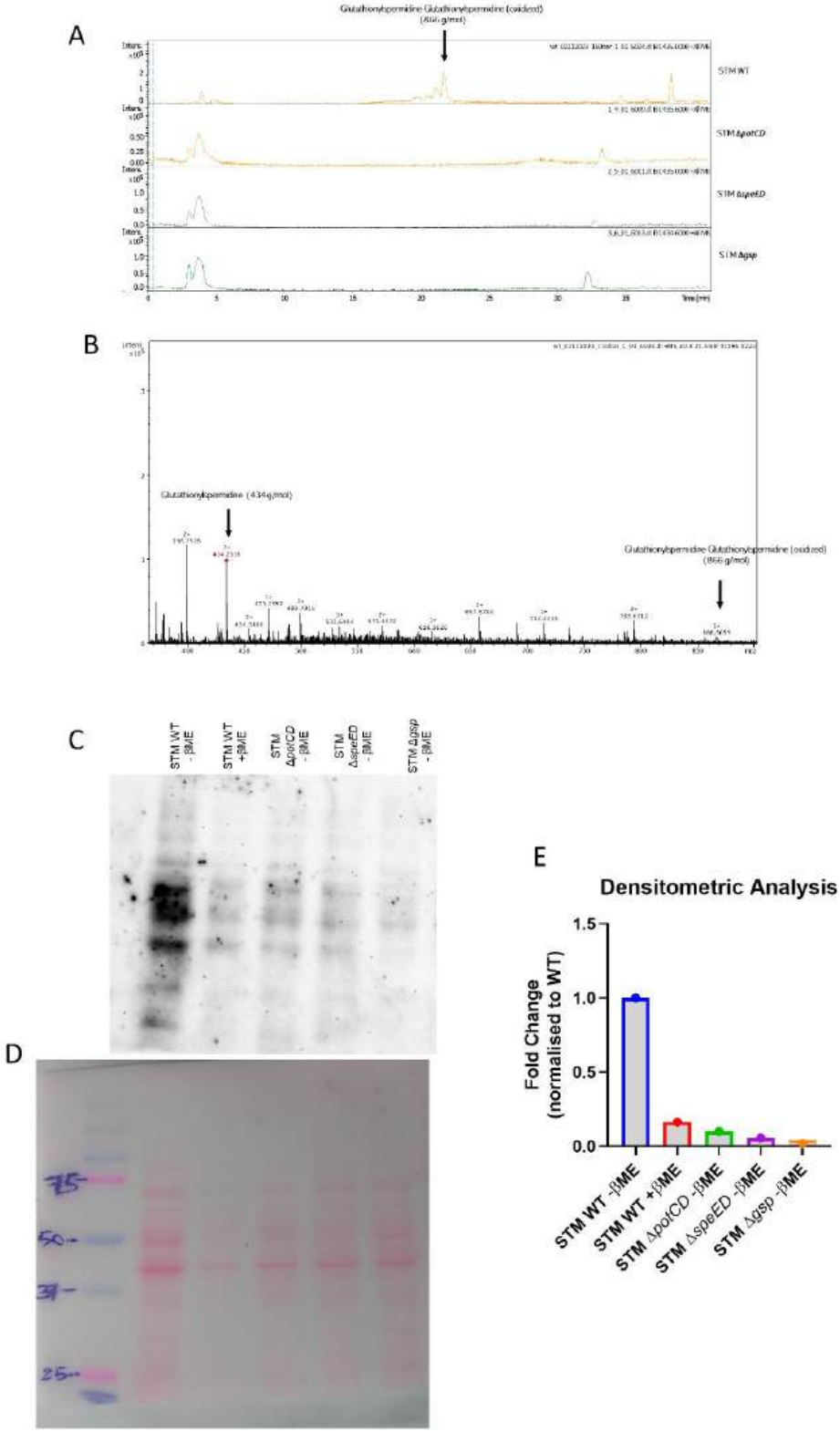

Figure S5: Spermidine regulates GspSA in *Salmonella* Typhimurium

A. The Extracted Ion Chromatogram(EIC) of oxidized Glutathinylspermidine in STM WT, STM Δ*potCD*, STM Δ*speED* and STM Δ*gsp,*the EIC of 435g, B. The mass spectrum showing presence of the oxidized Glutathinylspermidine (866 g/mol) in STM WT sample, C. The immunoblotting for GS-sp-thiolated proteins in STM WT, STM WT+beta mercaptoethanol, STM Δ*potCD*, STM Δ*speED* and STM Δ*gsp* upon exposure to 1mM hydrogen peroxide (anti-spermidine antibody), D. The Ponceau S stain for the above blot in C, E. Densitometric analysis for C. All data are represented as mean±SD from three independent experiments (N≥3).

Figure S6: GspSA is critical for *Salmonella* Typhimurium survival in macrophages

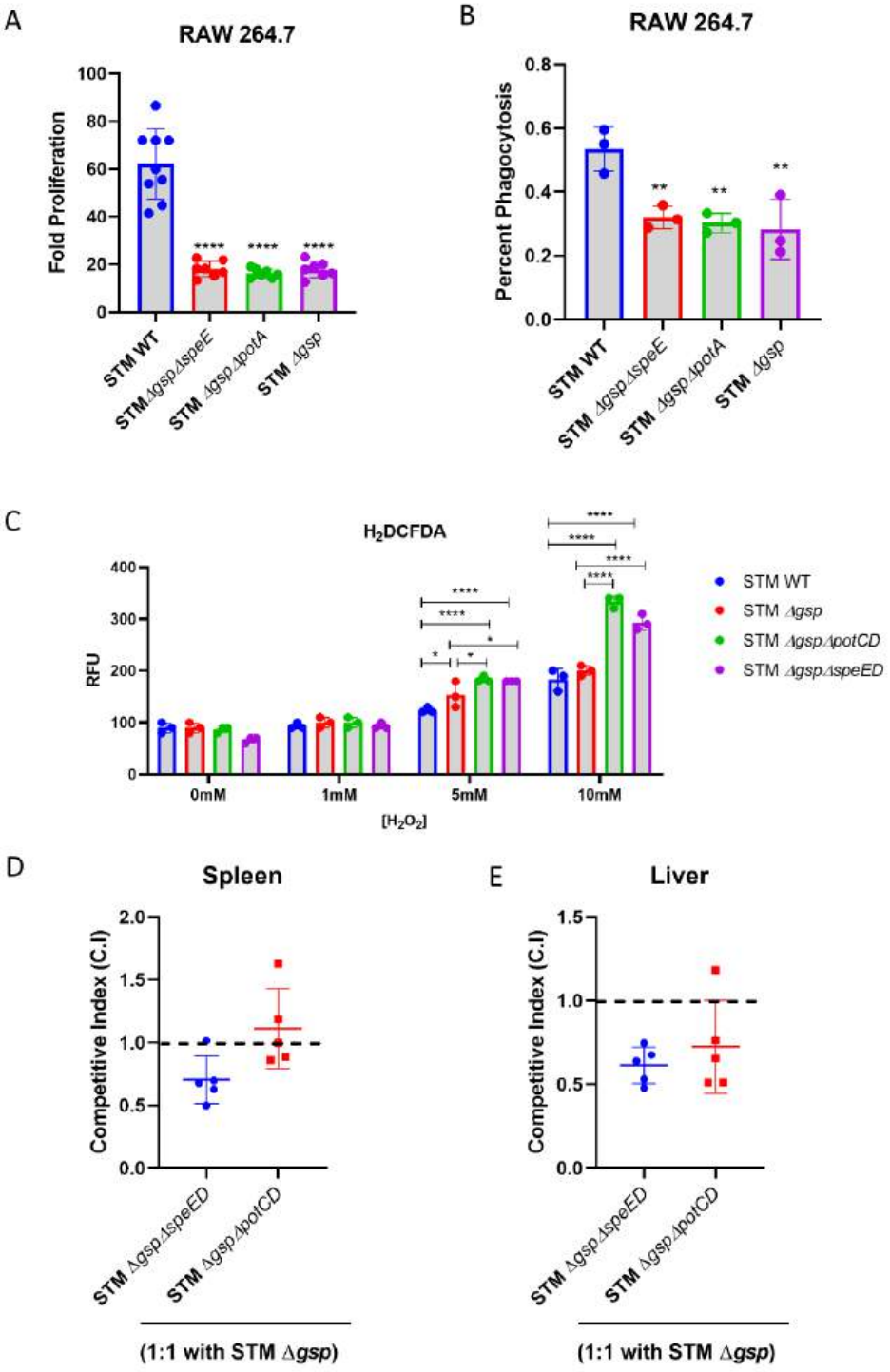

Figure S6: GspSA is critical for *Salmonella* Typhimurium survival in macrophages

A. The fold proliferation of spermidine and *gsp* double mutant strains in RAW264.7 cells (data is from one experiment representative of 3 independent experiments), B. The percentage phagocytosis of spermidine and *gsp* double mutant strains in RAW264.7 cells, C. The intracellular reactive oxygen species determination using H2DCFDA of spermidine and *gsp* double mutant strains, D. The competitive index of spermidine and *gsp* double mutant strains with single *gsp* mutant (1:1 ratio) in Spleen, and E. Liver of C57BL/6 mice . One-way ANOVA with Dunnet's post-hoc test was used to analyze the data; p values ****<0.0001, ***<0.001, **<0.01, Mann-Whitney was used to analyse animal experimental data, p values ****<0.0001, ***<0.001, **<0.01. All data are represented as mean±SD from three independent experiments (N≥3).

Figure S7: Spermidine mutants colonise less and lead to less liver tissue damage in C57B/L6J mice

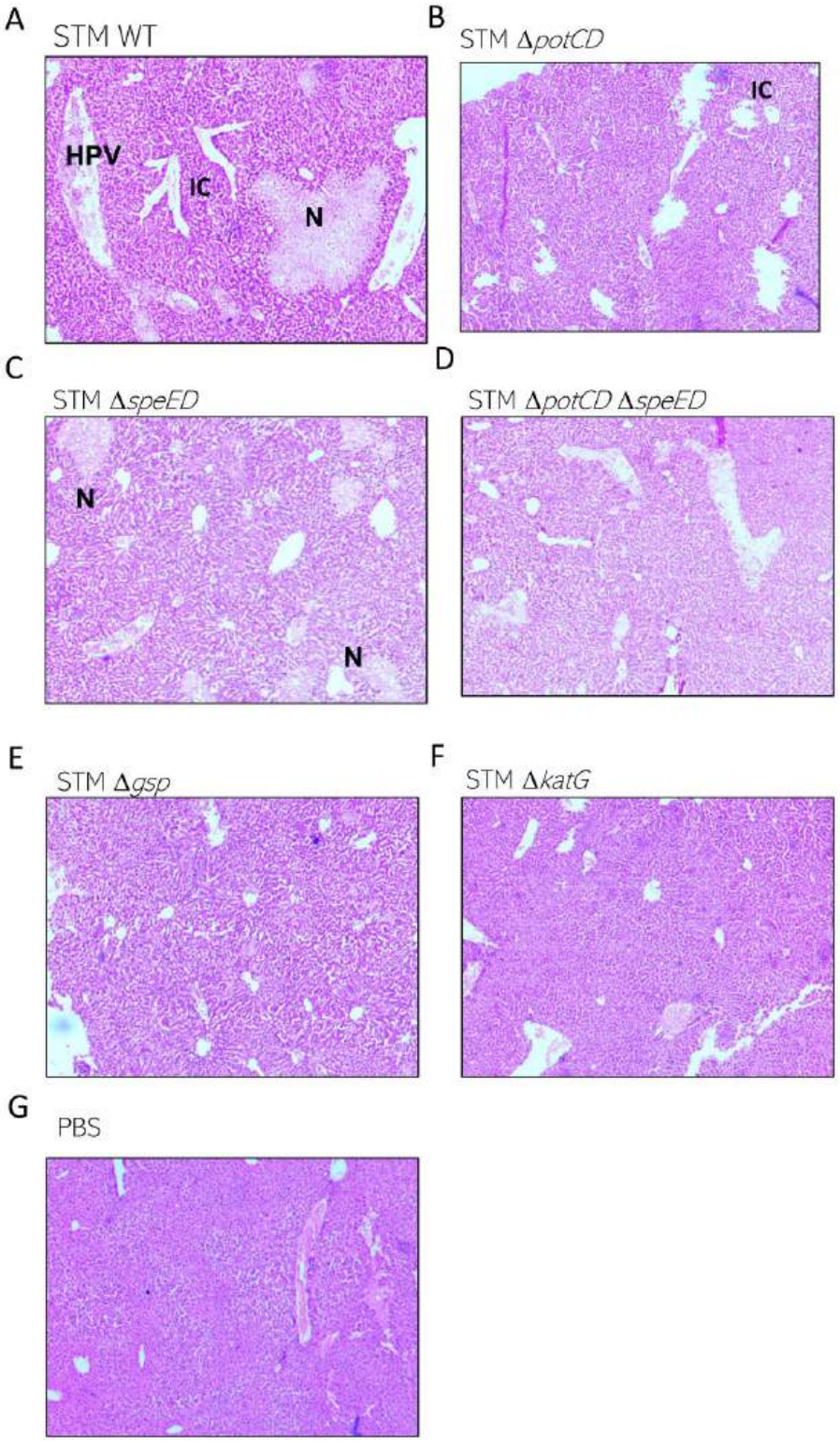

Figure S7: Spermidine mutants colonise less and lead to less liver tissue damage in C57B/L6J mice

The H and E staining of liver sections shows disease pathology (N=5, scale bar- 50μM). Data was acquired 3 days post infection intraperitoneally. Here, (IC) Multiple aggregations of inflammatory cells dispersed in the liver parenchyma, (N) shows several small necrotic areas, (C) congestion and damage to the endothelial lining of the central vein, (HPV) congestion of the hepatic portal vein.

Figure S8: Knockdown of Odc1 and Srm in macrophages adversely affect *Salmonella* Typhimurium survival

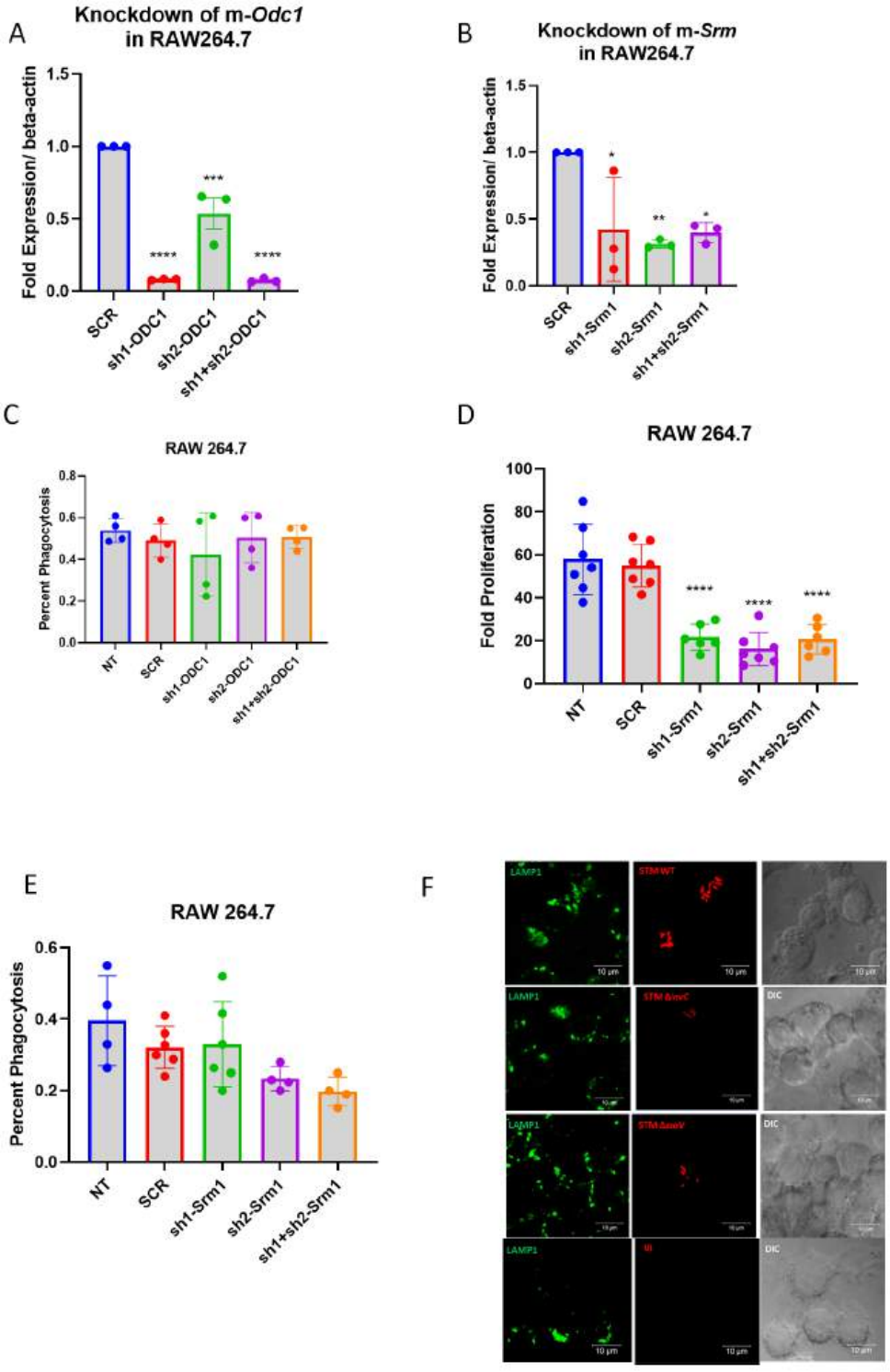

Figure S8: Knockdown of Odc1 and Srm in macrophages adversely affect *Salmonella* Typhimurium survival

A. Confirmation of knockdown of Odc1 in RAW264.7 cells using qRT-PCR, B. Confirmation of knockdown of Srm in RAW264.7 cells using qRT-PCR, C. The percentage phagocytosis of STM WT in RAW264.7 cells upon transient knockdown of Odc1, D. The fold proliferation of STM WT in RAW264.7 cells upon transient knockdown of Srm (data is from one experiment representative of 3 independent experiments), E. The percentage phagocytosis of STM WT in RAW264.7 cells upon transient knockdown of Srm (data is from one experiment representative of 3 independent experiments). Here SCR is Scrambled (no target for knockdown), two different targeted shRNA were used for knockdown purposes, Sh1is shRNA-1 for knockdown, Sh2 is shRNA-2 for knockdown, and Sh1+Sh2 indicates where both the shRNAs were used to obtain the knockdown, NT is untransfected F. Immunofluorescence imaging to study the spermidine in RAW 264.7 cells upon infection with STM WT, STM Δ*invC,* STM Δ*ssaV*, here green is Anti-mouse LAMP1(Alexa fluor 488), Red is pFPV-M-cherry expressing *Salmonella* strains, magenta is anti-Spermidine (Alexa fluor 647) and UI- uninfected. One-way ANOVA with Dunnet's post-hoc test was used to analyze the data; p values****<0.0001, ***<0.001, **<0.01, *<0.05. All data are represented as mean±SD from three independent experiments (N≥3).

Figure S9: Inhibition of polyamine biosynthesis in macrophages enhances nitric oxide production and attenuates *Salmonella* survival

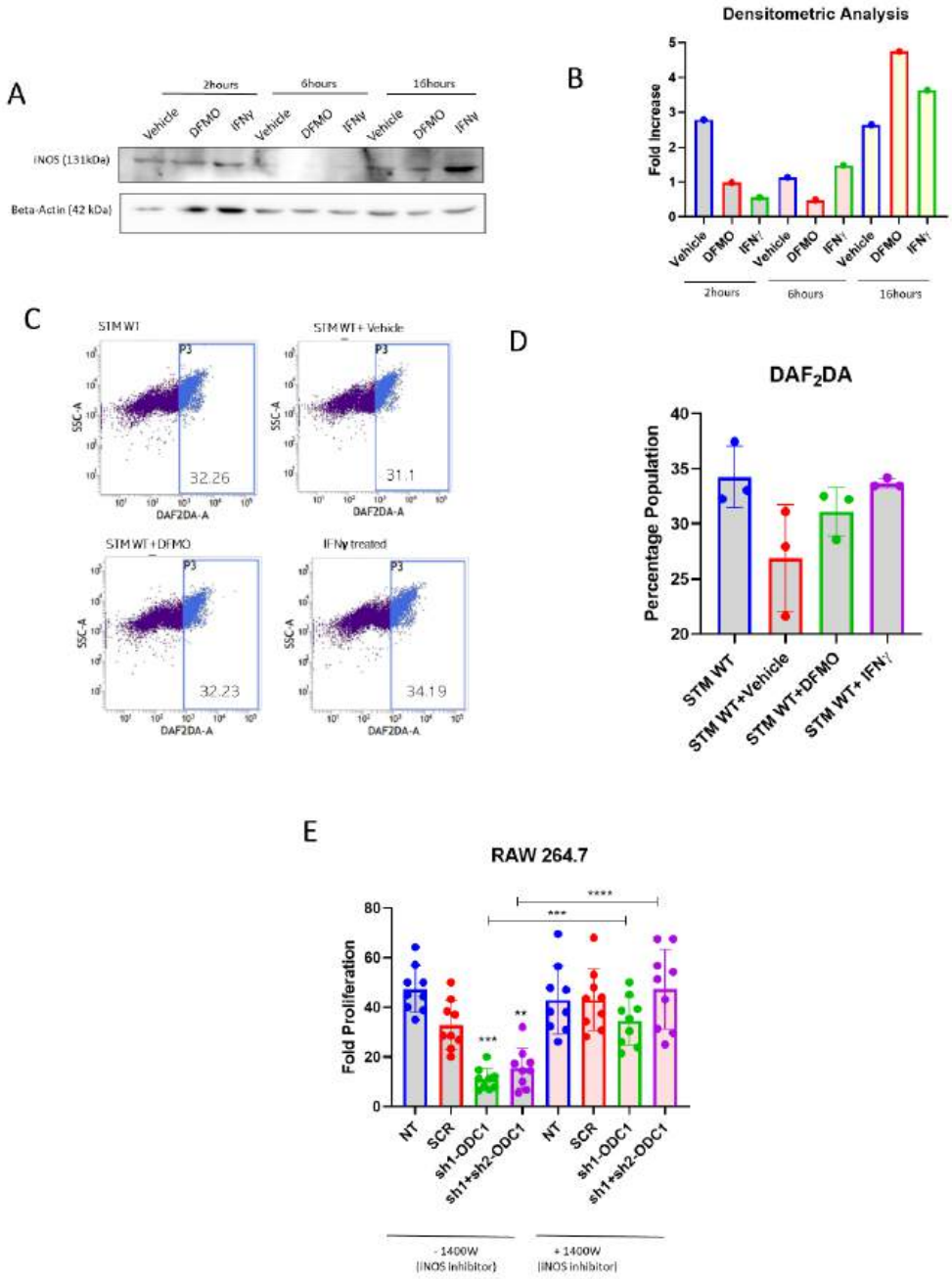

Figure S9: Inhibition of polyamine biosynthesis in macrophages enhances nitric oxide production and attenuates *Salmonella* survival

A. The western blot to study the expression of mNos2 in RAW264.7 cells upon infection with STM WT, B. the densitometric analysis of (A), C. DAF_2DA staining to study the nitric oxide production in RAW264.7 cells upon infection with STM WT and treatment of iNOS inhibitor (1400W dihydrochloride, 5μM) to all sets, D. Quantification of (C), E. Fold proliferation of STM WT in RAW264.7 cells upon knockdown of Odc1 and treatment with iNOS inhibitor (1400W dihydrochloride, 5μM) (data is from one experiment representative of 3 independent experiments). Here SCR is Scrambled (no target for knockdown), two different targeted shRNA were used for knockdown purposes, Sh1is shRNA-1 for knockdown, Sh2 is shRNA-2 for knockdown, and Sh1+Sh2 indicates where both the shRNAs were used to obtain the knockdown, NT is untransfected. One-way ANOVA with Dunnet's post-hoc test was used to analyze the data; p values ****<0.0001, ***<0.001, **<0.01, *<0.05. All data are represented as mean±SD from three independent experiments (N≥3).

Figure S10: DFMO is able to control *Salmonella* Typhimurium colonisation in mice

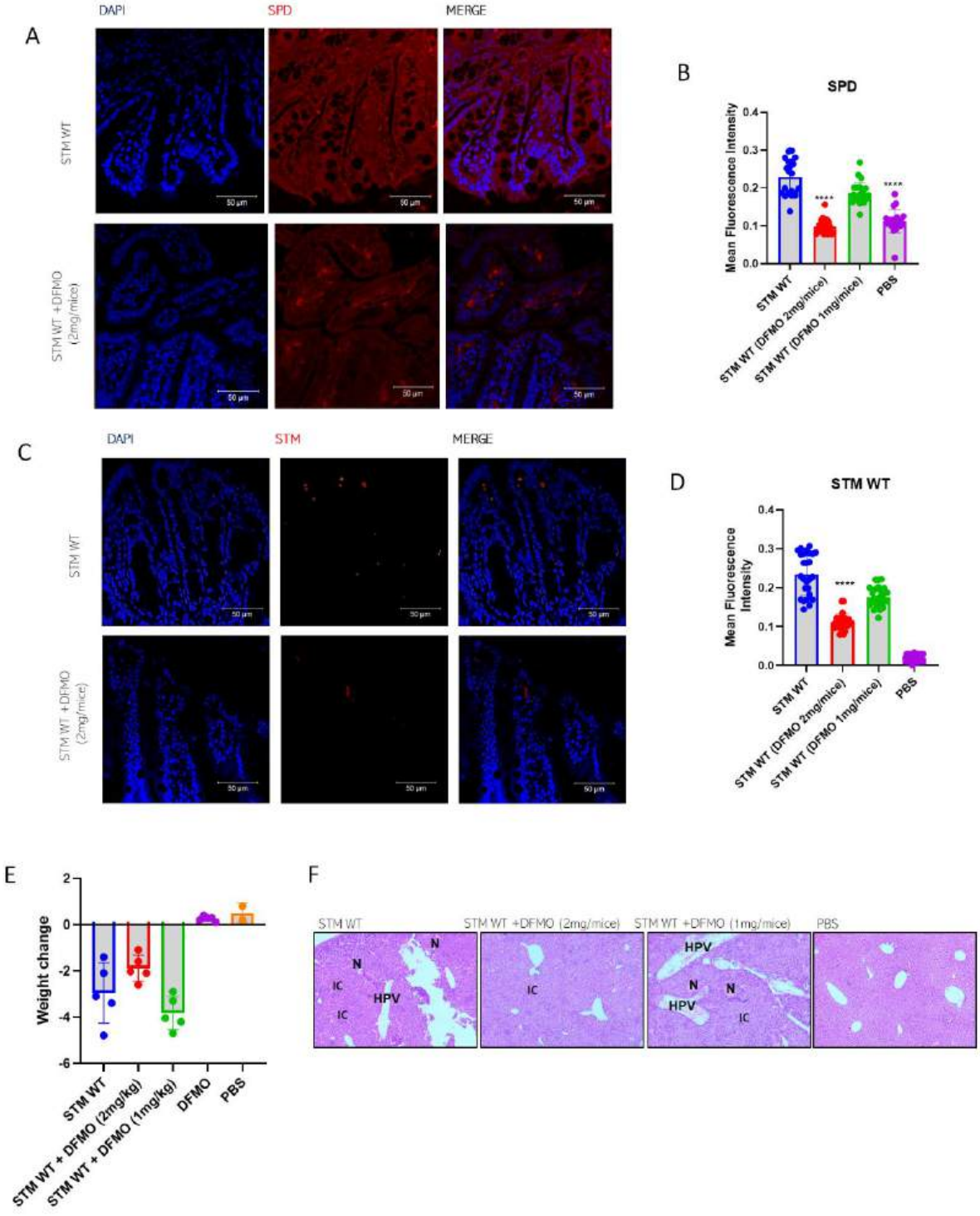

Figure S10: DFMO is able to control *Salmonella* Typhimurium colonisation in mice

A. Immunofluorescence imaging of mice ileum showing the inhibitory effect of DFMO on polyamine biosynthesis in mice. Here DAPI(blue) stains the intestinal cells and Anti-spermidine antibody is used to stain for spermidine (Cy3 tagged secondary antibody (red)). Representative images are shown, B.The quantification of (A) by Mean fluorescence intensity (data is from one experiment representative of 3 independent experiments), C. Immunofluorescence imaging of mice ileum showing the colonisation of STM in mice upon DFMO treatment. Here DAPI(blue) stains the intestinal cells, and Anti-*Salmonella*-LPS antibody is used to stain for STM (Cy3 tagged secondary antibody (red)). Representative images are shown , D. The quantification of (C) by Mean fluorescence intensity (the representative image of one time experiment of N=3, n=>25 plotted as ±SD), E. The weight change (reduction) of mice upon infection with STM WT and followed the intraperitoneal treatment of DFMO (2mg/kg and 1mg/kg of body weight) every alternate day. F. The H and E staining of liver sections showing disease pathology (N=5, scale bar-50μM). Data acquired 5 days post infection. Here, (IC) Multiple aggregations of inflammatory cells dispersed in the liver parenchyma, (N) shows several small necrotic areas, (C) congestion and damage to the endothelial lining of the central vein, (HPV) congestion of the hepatic portal vein. One-way ANOVA with Dunnet's post-hoc test was used to analyze the data ; p values ****<0.0001, ***<0.001, **<0.01, *<0.05. All data are represented as mean±SD from three independent experiments (N≥3).

Ethics statement

All the animal experiments were approved by the Institutional Animal Ethics Committee, and the guidelines provided by The Committee for the Purpose of Control and Supervision of Experiments on Animals (CPCSEA, a statutory Committee, established under Chapter 4, Section 15(1) of the Prevention of Cruelty to Animals Act 1960) and by National Animal Care were strictly followed

during all experiments. (Registration No: 435 48/1999/CPCSEA). The approved protocol number is CAF/Ethics/852/2021.

Acknowledgement

Prof. Amit Singh is duly acknowledged for providing us with the *iNOS* knockout mice. Prof. G. Subba Rao from MCB, IISc, is duly acknowledged for providing shRNA plasmid clones for knockdown generation. Divisional Mass Spectrometry facility IISc and Mrs. Sunita Joshi for the MS analysis. Departmental Confocal Facility. Departmental Real-Time PCR Facility, Divisional Flowcytometry Facility and Central Animal Facility at IISc are duly acknowledged. Mr Sumith and Ms Navya are acknowledged for their help in image acquisition. Dr. Ritika Chatterjee and Mr Anirban Roy is acknowledged for critical reading of the manuscript. Mr Amartya Mukherjee, Ms Rhea Vij, Mr Sushovan Bhattacharyya and Ms Bhavya Joshi are also acknowledged for technical help.

Author contribution statement

AVN and DC conceived the study. AVN and DC designed experiments. AVN and AS performed experiments. RSR analysed for the disease score of tissue samples. AVN analyzed the data, prepared the figures and wrote the manuscript draft. AVN, AS and DC reviewed and edited the manuscript. DC supervised the work. All the authors read and approved the manuscript.

Funding

This work is supported by the Department of Biotechnology (DBT), Ministry of Science and Technology, the Department of Science and Technology (DST), Ministry of Science and

Technology. DC acknowledges DAE-SRC ((DAE00195) outstanding investigator award and funds and ASTRA Chair Professorship funds. The authors jointly acknowledge the DBT-IISc partnership program. Infrastructure support from ICMR (Center for Advanced Study in Molecular Medicine), DST (FIST), UGC-CAS (special assistance), and TATA fellowship is duly acknowledged. AVN acknowledges the IISc-MHRD for financial assistance, and AS acknowledges UGC for financial assistance. RSR acknowledges IISc for the financial help.

Conflict of Interest

The authors declare no conflict of interest.